ANL-5657
Progress Reports

ARGONNE NATIONAL LABORATORY
P. O. Box 299
Lemont, Illinois

REACTOR ENGINEERING DIVISION QUARTERLY REPORT

SECTION II

July, August, September, 1956

Compiled by
Members of the Reactor Engineering Division

December, 1956

Operated by The University of Chicago
under
Contract W-31-109-eng-38

DISCLAIMER

TABLE OF CONTENTS

Page

PART A. ADVANCED WATER REACTOR PROGRAM

SUMMARY 5

PART B. FAST BREEDER REACTOR PROGRAM

SUMMARY 7

I. EXPERIMENT BREEDER REACTOR-II (EBR-II) 9

A. Coolant Flow Characteristics of Primary System. 9
B. Reactor Temperatures and Fuel Expansions Resulting from Exponential Power Excursions in EBR-II 11
C. 10,000-gpm, d-c Electromagnetic Pump, Homopolar Generator and Test Loop 21
D. 5,000-gpm, a-c Linear Induction Pump and Test Loop. 22
E. 5,000-gpm, Mechanical Sodium Pump and Test Loop. 24
F. Rotating Plug Seal Test 33

II. SUPPORTING AND ALTERNATE DESIGN RESEARCH AND DEVELOPMENT 35

A. S_4 Calculations to Investigate Inhomogeneities in ZPR-III Assemblies 35
B. Effect of High Temperature on Irradiated Fissium Alloy . . . 55
C. Evaluation of Gears and Bearings for Service in Sodium at Elevated Temperatures 57
D. Bellows Seal and Sodium Condensation Test 57
E. Sodium-Air Reaction Experiments. 57

LIST OF FIGURES

No.	Title	Page
1	Schematic of EBR-II Primary System.	10
2	Flow Rate Through Reactor vs Flow Rate Through Operating Main Pump for Various Modes of Pump Operation	12
3	Primary System Pressure Drop Relative to Flow Through Reactor.	13
4	Main Pump Head vs Flow Rate Through Operating Main Pump Based on Full Rectifier Voltage Applied to Pump (A).	14
5	Flow Rate Through Reactor vs Main Pump Rectifier Voltage	15
6	Flow Rate Through Reactor vs Main Pump Rectifier Current.	16
7	Main Pump Rectifier Voltage vs Current Input	17
8	Effect of Step Change of Rectifier Voltage on Main Pump on Reactor Coolant Outlet Temperature	18
9	Ratio of Integrated Power to Fractional Change in Fuel Length as a Function of Reactor Period with No Coolant Flow	19
10	Ratio of Integrated Power to Fractional Change in Fuel Length as a Function of Reactor Period with Coolant Flow at 26 fps.	20
11	Homopolar Generator	22
12	d-c Electromagnetic Pump - Homopolar Generator Test Loop	23
13	5,000-gpm, a-c Linear Induction Pump - Test Loop	25
14	Thermal Insulation Being Applied Over Tack Welded Carbon Steel Cladding	26

LIST OF FIGURES

No.	Title	Page
15	5,000-gpm Mechanical Sodium Pump	28
16	Section of 5,000-gpm Mechanical Sodium Pump	29
17	Appearance of (A) Pump Impeller and Sodium Bearing Surface and (B) Hydraulic Bearing Shell Following Manufacturer's Test With Water as Circulating Fluid	30
18	Performance Characteristics of 5,000-gpm Mechanical Pump With Water as Circulating Fluid	31
19	5,000-gpm Mechanical Pump Test Loop	32
20	Rotating Plug Seal	34
21	Schematics of Drawer Loadings	41
22	Comparison of Measured With Calculated Fission Rates (Problems No. 9 and No. 10)	43
23	Comparison of Measured With Calculated Fission Rates (Problems No. 3 and No. 8)	44
24	Spatial Distribution of Fission Rates and Total Flux in Assembly 2A	47
25	Spatial Distribution of Fission Rates and Total Flux in Assembly 2E	48
26	Schematics of Drawer Loadings For Proposed Critical Assemblies	49
27	Spatial Distribution of Fission Rates and Total Flux (PBR Analysis: Problem No. 15)	51
28	Spatial Distribution of Fission Rates and Total Flux (PBR Analysis: Problem No. 16)	52
29	Spatial Distribution of Fission Rates and Total Flux (PBR Analysis: Problem No. 17)	53
30	Spatial Distribution of Fission Rates and Total Flux (PBR Analysis: Problem No. 18)	54

LIST OF FIGURES

No.	Title	Page
31	Test Apparatus Used to Evaluate Rotary Seals, Gears and Bearings for Liquid Metal-Cooled Systems	58
32	Bellows Failure Which Occurred After 40,000 Cycles at Room Temperature, With Internal Argon Gas Pressure of 15-30 in. H_2O	62
33	Sodium-Air Reaction Test Facility.	64
34	Mortar Subassembly	65
35	Typical Oscillographic Pressure Transient Characteristics	67

LIST OF TABLES

No.	Title	Page
I	Summary of Calculated Parameters for S_4 Analysis . . .	45
II	Heating Tests on CP-5-7 Fissium Alloy Pins.	56
III	Summary of Gear Tests in Liquid Sodium	59
IV	Summary of Ball Bearing Tests in Liquid Sodium and Sodium Vapor.	60
V	Summary of Tests on Various Journal Bearing - Shaft Combinations in Liquid Sodium	61
VI	Peak Pressure Variation with Sodium Quantity.	66

REACTOR ENGINEERING DIVISION QUARTERLY REPORT

SECTION II

July, August, September, 1956

PART A. ADVANCED WATER REACTOR PROGRAM

A large portion of the Reactor Engineering Division effort on the Advanced Water Reactor Program during this quarter was directed toward the early completion of the Experimental Boiling Water Reactor (EBWR) facility. Most of the work involved completion of fabrication, installation, and checking out of equipment. Therefore, the usual detailed quarterly report is omitted for this quarter, and the present brief summary is substituted. Details of significant events will appear in the regular Quarterly Report for October, November, and December, 1956.

The production of fuel plates for EBWR has been completed by the Metallurgy Division; about 900 plates were made. To date about 75 fuel assemblies have been completed from these plates. Corrosion testing has been accomplished to the extent of sufficient plates for the entire core, as well as for 60 of the assemblies.

The turbine shell and diaphragms and main steam piping have been plated with nickel by the Kanigen Process. The turbine has been reassembled, installed in the plant, and welded to the condenser. The steam piping and steam dryer-emergency cooler have also been installed in the plant; the hydrostatic testing has been completed on this portion of the system. Other components completely installed include the second reactor feedwater pump, the demineralized water storage tank, the start-up heater, the steam by-pass valve and its control system, the nuclear instrument tubes, and the 20-ton building crane. The ion exchange vessels for the reactor purification system have been received and lead shielding has been applied.

The reactor vessel insulation has been installed and all shielding has been completed with the exception of pipe tunnels. The vessel cover and initial sets of gaskets have been received. Internal components, such as the thermal shield and core support grid plate, have been "trial fitted" in the vessel and removed for rework. All piping connections to the reactor have been completed to points outside the shield.

In the power-plant area, the concrete ceiling of the main floor was poured, air-conditioning units were installed, and the exterior insulation of the steel shell was completed. All masonry and roofing of the service building have been finished.

Outdoor transformers and switchgear were placed in position. Installation of the cooling tower was completed except for minor equipment.

Supporting research and development activities have been carried forward on a reduced scale because of manpower demands for EBWR. The progress in this work will be included in the Quarterly Report for the period ending December, 1956.

PART B. FAST POWER BREEDER REACTOR PROGRAM

SUMMARY - L. J. Koch

The Architect-Engineer Contract Board reviewed the proposals submitted by qualified firms desiring to carry out the architect-engineer work for the EBR-II Plant. They selected the most qualified firm to conduct this work and made these recommendations to the Laboratory management. It is expected that a contract will be negotiated early in the next quarter and that the construction design work for EBR-II will be initiated.

The construction of the large pipe test loops (12-inch, Schedule 10 piping) was essentially completed in the Liquid Metals Mock-up Building (D-308). The equipment to be tested consists of prototype components for the EBR-II Plant. The 5,000-gpm centrifugal pump and the 5,000-gpm, a-c electromagnetic linear induction pump were received and installed in their respective test loops. These units have a rated capacity equivalent to the requirements of the EBR-II secondary sodium system. Each will be tested under conditions simulating the anticipated operating conditions of the secondary system. The arrangement of the EBR-II secondary system will permit the use of either of these units, and provisions may be included to permit incorporating one of each type of pump in parallel in the system. The 10,000-gpm, d-c electromagnetic pump is being constructed in place in the Liquid Metals Mock-up Building. It also includes a sodium test loop. This pump will be tested in conjunction with the 250,000-ampere homopolar generator. The pump and generator have been designed as a package unit. In addition to the pump data, the tests will provide information on pumping system components required for EBR-II.

Each of the test loops includes a stainless steel, 12-inch, bellows-sealed, wye-type valve. The pump testing program will afford an excellent opportunity to establish the reliability and performance of this particular design of valve. Each loop includes flow- and pressure-measuring instrumentation appropriate for use in the EBR-II system. Included will be electromagnetic flowmeters which have not been heretofore employed in 12-inch pipe systems.

Three different heating systems are being employed on the pipe loops to maintain the sodium above its freezing point. The a-c induction pump loop employs 60-cycle induction heating; the centrifugal pump test loop is contained in a steel box which is heated by circulating hot air; and the d-c electromagnetic pump loop employs direct resistance wire wrapped around the pipe. The pump tube and the magnet are also heated by resistance heating. Operation of the two 5,000-gpm pump loops should begin during the next quarter. Preliminary testing of the homopolar generator and d-c pump is also scheduled to begin during the quarter.

The EBR-II Working Model continued to operate very satisfactorily. The d-c electromagnetic pump has operated approximately 4,000 hr with no difficulty. The system was shut down for a short time to install flow- and pressure-measuring instrumentation in the shutdown cooler loop to determine the operating characteristics of this equipment.

A program of analysis and experiment has been initiated to develop the required information to be included in the EBR-II Hazards Report. The analyses include various reactor transients, an estimate of the damage resulting from a maximum credible accident, and the containment of the energy release in the event of such an accident. An analysis of the expansion characteristics of the fuel element during a rapid transient has been completed. This is an important "shutdown mechanism" during a transient. An experimental apparatus has been constructed to determine the effects of sodium-oxygen reactions when sodium and air are mixed in different quantities and at different rates. These experiments will determine the maximum pressure and temperatures obtained when sodium is expelled into air in a closed container. A reaction of this type is possible if sodium is expelled into the reactor building as a result of a serious incident. It is hoped to determine the variables which affect the resultant pressures and temperatures. Preparation of the EBR-II Hazards Report will be initiated during the next quarter.

I. EXPERIMENTAL BREEDER REACTOR-II (EBR-II)

A. Coolant Flow Characteristics of Primary System - O. S. Seim, T. R. Spalding, R. A. Jaross

The EBR-II Design Study No. 2 provides for the use of three d-c electromagnetic pumps in the primary cooling system. Two pumps, located in the two coolant inlet lines to the reactor, operate in parallel and supply the bulk of the normal reactor coolant flow, each is termed a "main" primary pump and has an approximate capacity of 6,000 gpm of sodium at a head of 55 psi. Both are supplied power from (separate) metallic rectifiers. The third pump, located in the single outlet line from the reactor, operates in series with the two "main" pumps and supplies only a very small portion of the normal reactor coolant flow. The third pump is referred to as the "auxiliary" pump and has an approximate capacity of 500 gpm at a head of 0.15 psi. The chief function of the auxiliary pump is to reduce temperature excursions of the coolant during certain types of emergency scrams. This pump is normally supplied power from a rectifier, but, in the event of plant power failure, is driven by a battery floating on the line. The primary cooling system is shown schematically in Fig. 1. The entire system operates submerged in the bulk sodium of the primary tank.

A study has been made of the approximate steady-state flow characteristics of the primary system for several possible modes of pump operation which may be employed during: (1) normal reactor operation and shutdown; (2) abnormal reactor operation; (3) experimental operation; or (4) as a result of pump failures or other conditions beyond the operator's control. The information is essential both for evaluation of certain aspects of reactor control and for the formulation of specifications for the rectifiers used to supply power to the main pumps.

The modes of pump operation investigated were:

1. Pumps No. 1 and No. 2 operating.
2. Pumps No. 1, No. 2, and (A) operating on rectifier (normal reactor operation).
3. Pump No. 1 or No. 2 operating.
4. Pump No. 1 or No. 2, and (A) operating on rectifier.
5. Pump (A) operating on rectifier; no natural convection (normal reactor shutdown).
6. Pump (A) operating on battery, 1.7 volts; no natural convection assumed.
7. Pumps No. 1, No. 2, and (A) operating on battery, 1.7 volts; no natural convection assumed.
8. Pump No. 1 or No. 2, and (A) operating on battery, 1.7 volts; no natural convection assumed.

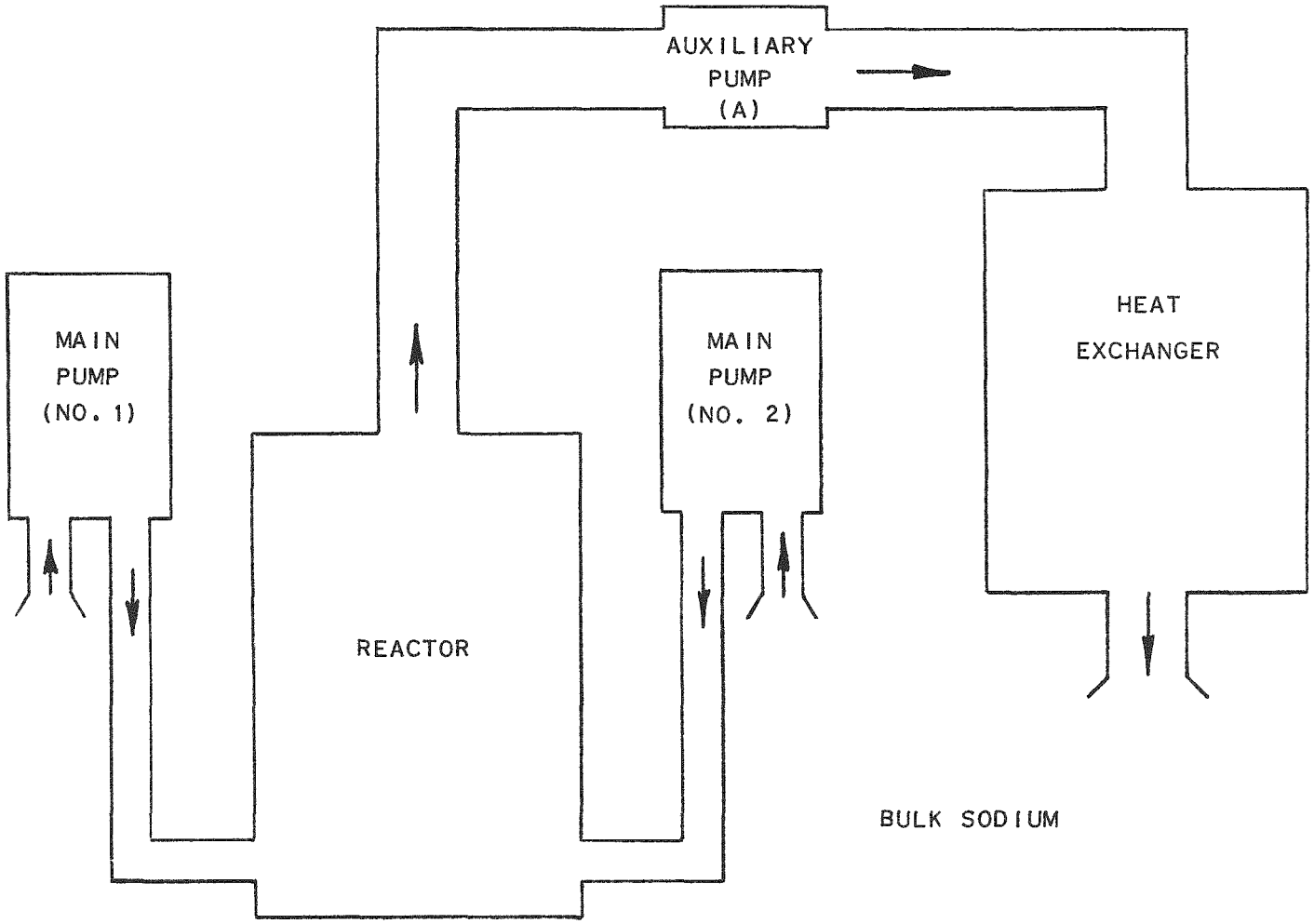

FIG. 1
SCHEMATIC OF EBR-II PRIMARY SYSTEM

RE-8-19564-A

The flow relationship between the operating "main" pump (or pumps) and that of the reactor is developed in Fig. 2. The resulting system pressure drops are presented relative to flow through the reactor in Fig. 3. The resultant requirements for pump head and flow rate for each main pump are shown in Fig. 4. Based on this, the approximate voltages and amperages for each of the main pump rectifiers versus flow rate through the reactor were calculated; these are shown in Figs. 5 and 6, respectively. The approximate range of rectifier current for a main pump associated with any rectifier voltage for the entire range of pump operation modes is shown in Fig. 7.

During reactor operation, it is desired that the average temperature of the reactor coolant (or, qualitatively, the coolant outlet temperature) change by as small an amount as possible with any incremental change in the rectifier voltage of the main pump. To enable calculation of the maximum magnitude of increment of rectifier voltage permissible throughout the voltage range, the relation between the change of outlet coolant temperature (at constant reactor power) versus flow rate through the reactor for various magnitudes of voltage increment was determined. These results are given in Fig. 8.

Specifications for the main pump rectifiers have been completed on the basis of the above. Invitations to bid on the construction of one rectifier have been let.

B. Reactor Temperatures and Fuel Alloy Expansions Resulting From Exponential Power Excursions in EBR-II - T. R. Bump, and R. W. Seidensticker

When excess reactivity is suddenly added to a reactor, the reactor power rises exponentially with consequent increase in internal reactor temperatures. One effect of an increase in reactor temperature in the case of EBR-II is longitudinal expansion of the fuel. Such fuel expansion causes a decrease in reactivity; i.e., it reduces the effect of the original reactivity addition. Consequently, determination of the amount of expansion to be expected under various conditions is of great importance in evaluation of the over-all reactor shutdown characteristic operative in any postulated excursion.

A study has been made of the temperature of fuel alloy (and coolant sodium) and the longitudinal expansion of the fuel for the following important cases:

1. No coolant flow: Initial fuel and coolant temperatures the same as those anticipated during loading and unloading operations (about 600F); initial reactor power, 1 watt; excursion periods from 10^{-5} to 10^{-2} second (see Fig. 9).

RE-7-19634-A O.S.SEIM:G.K.,2-4-57

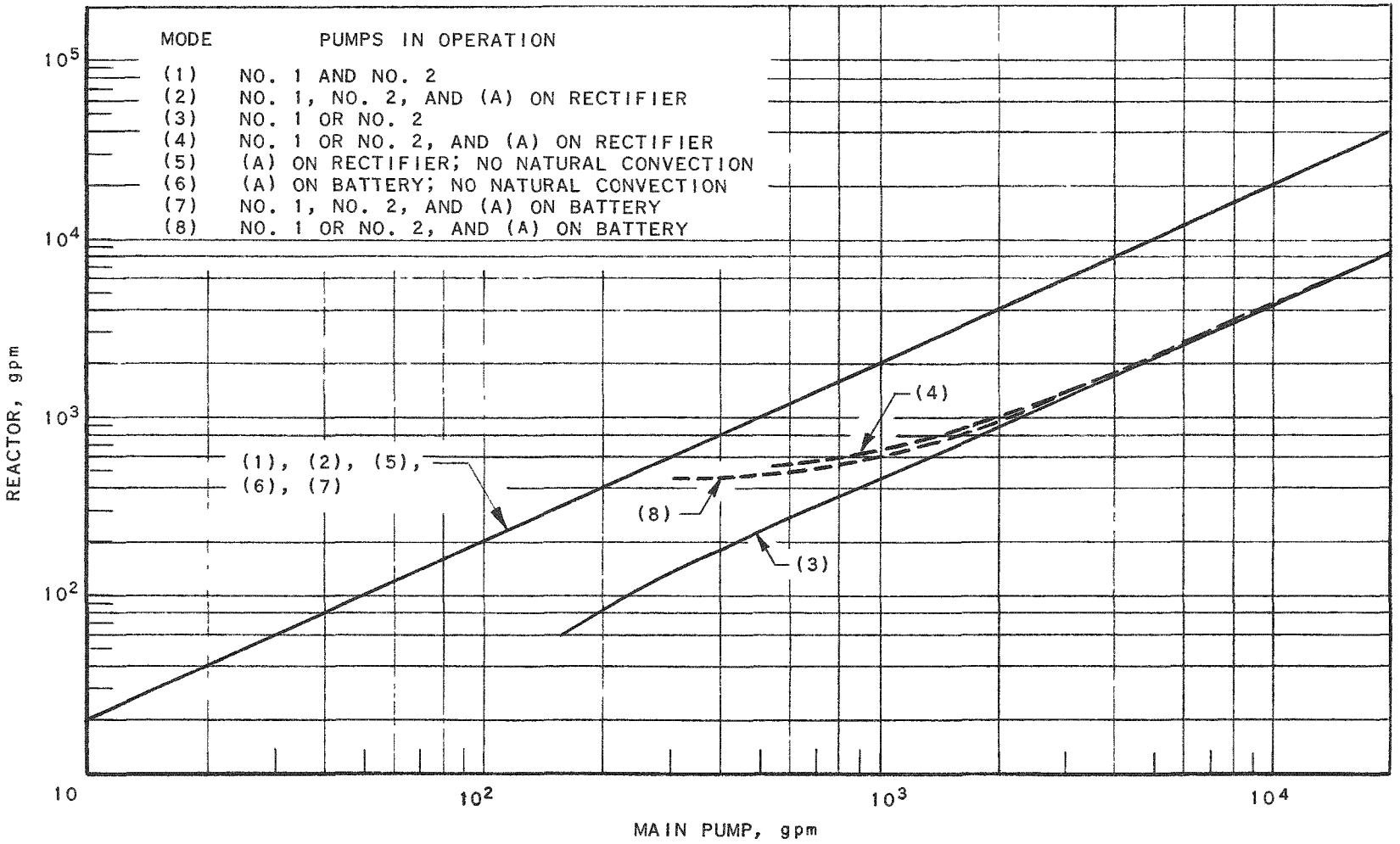

FIG. 2
FLOW RATE THROUGH REACTOR VS FLOW RATE THROUGH OPERATING MAIN PUMP FOR VARIOUS MODES OF PUMP OPERATION

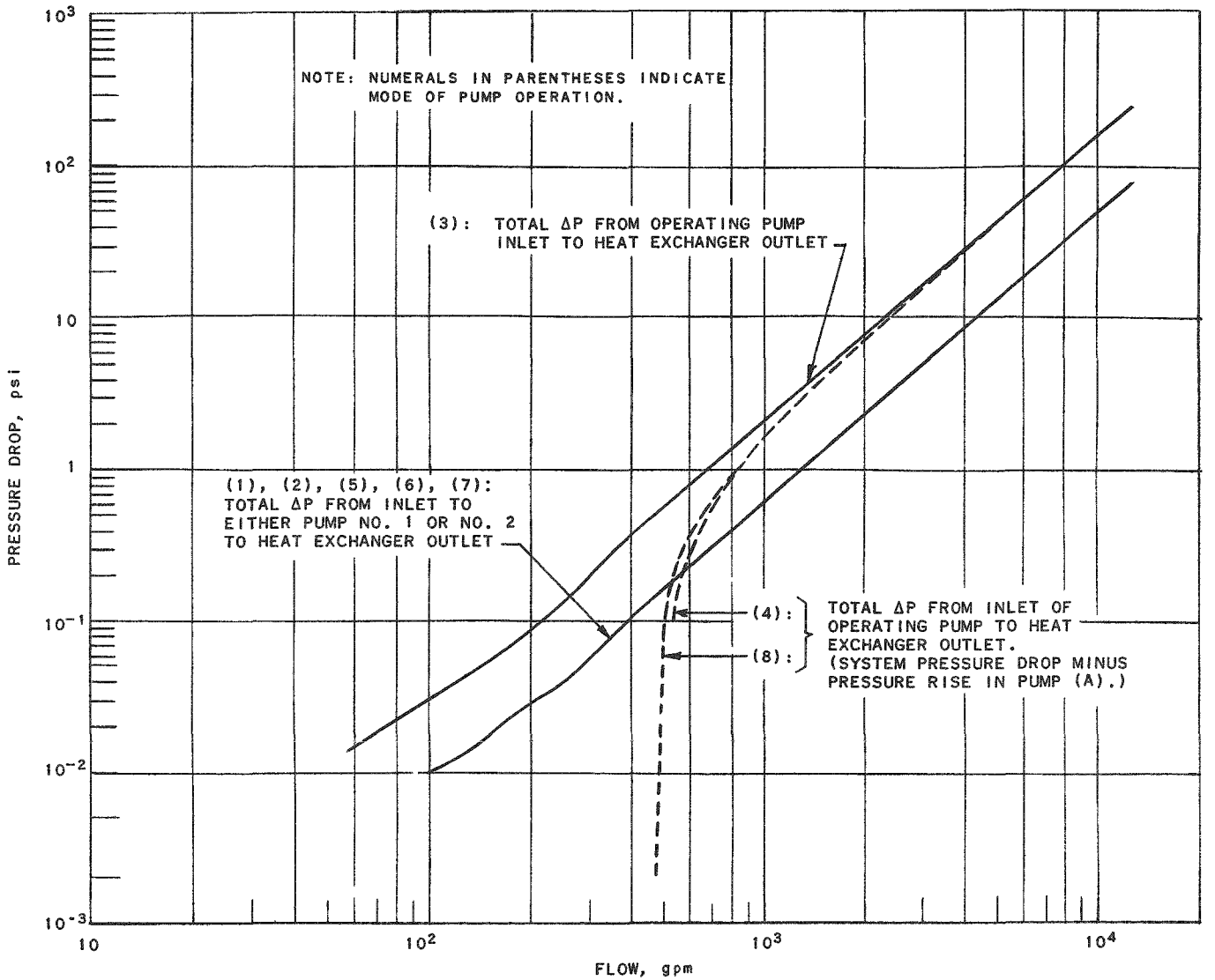

FIG. 3
PRIMARY SYSTEM PRESSURE DROP RELATIVE TO FLOW THROUGH REACTOR

RE-7-19633-B

RE-7-19641-B

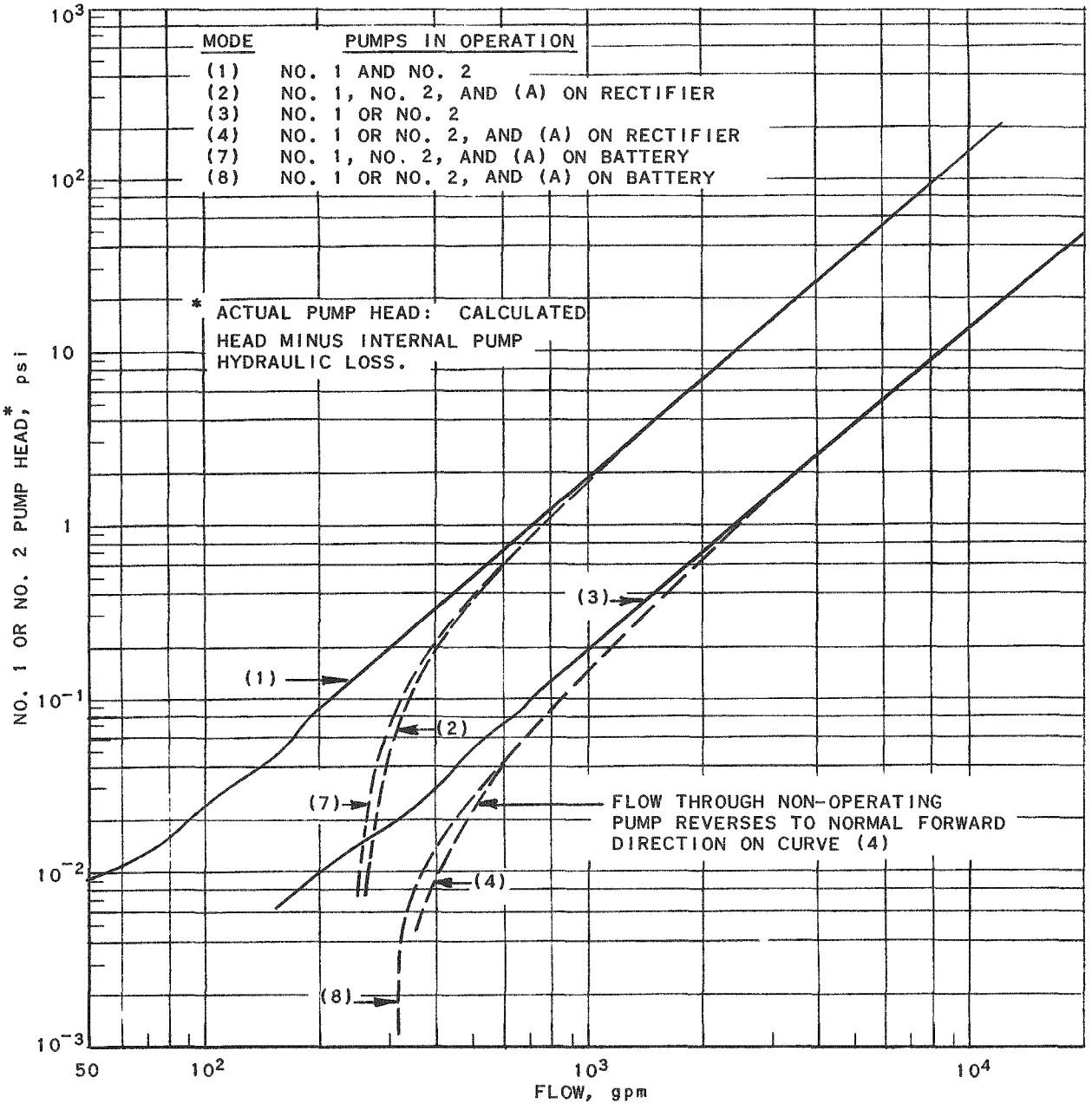

FIG. 4
MAIN PUMP HEAD VS FLOW RATE THROUGH OPERATING MAIN PUMP.
BASED ON FULL RECTIFIER VOLTAGE APPLIED TO PUMP (A)

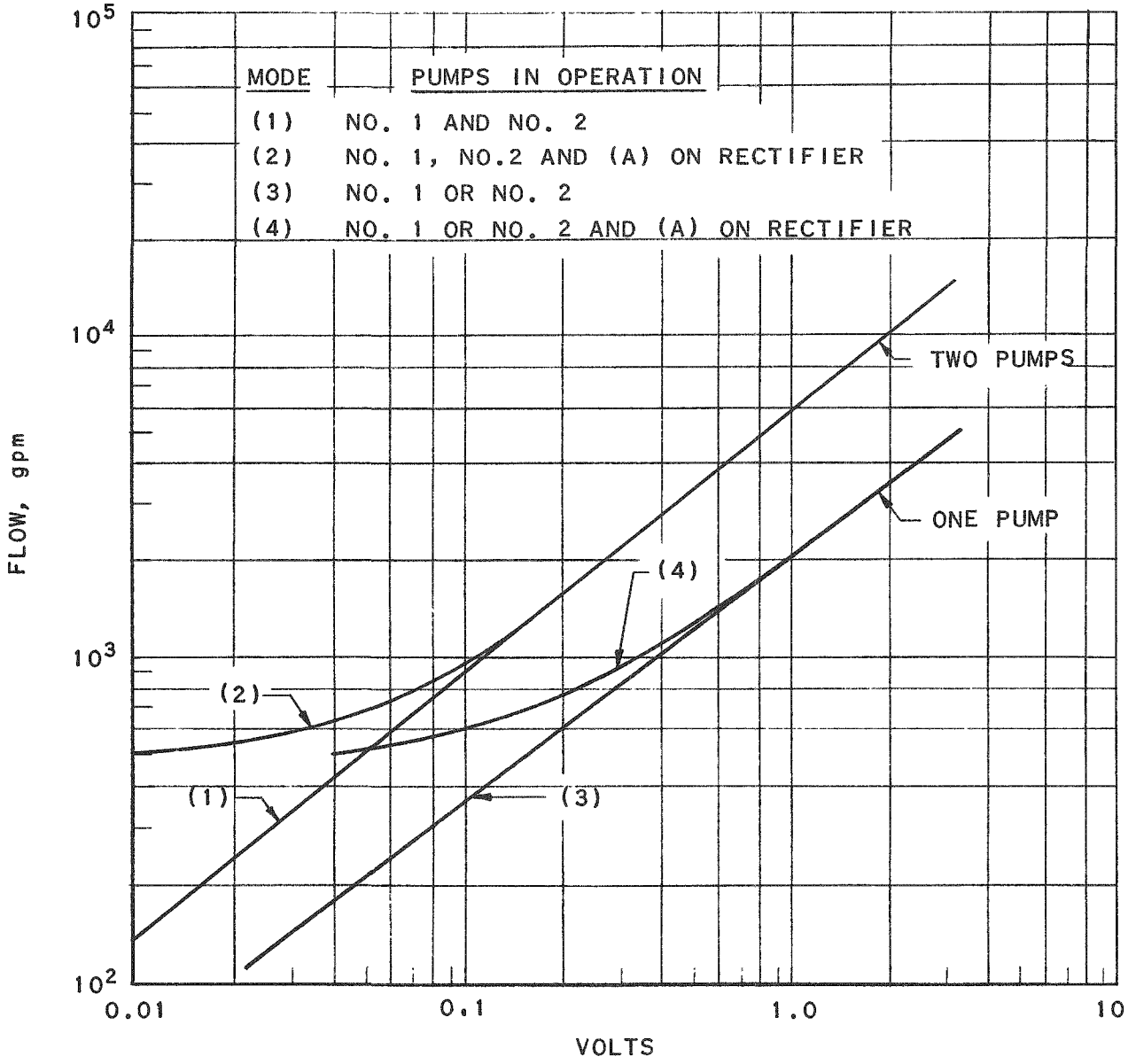

FIG. 5
FLOW RATE THROUGH REACTOR VS MAIN PUMP RECTIFIER VOLTAGE

RE-7-19599-A

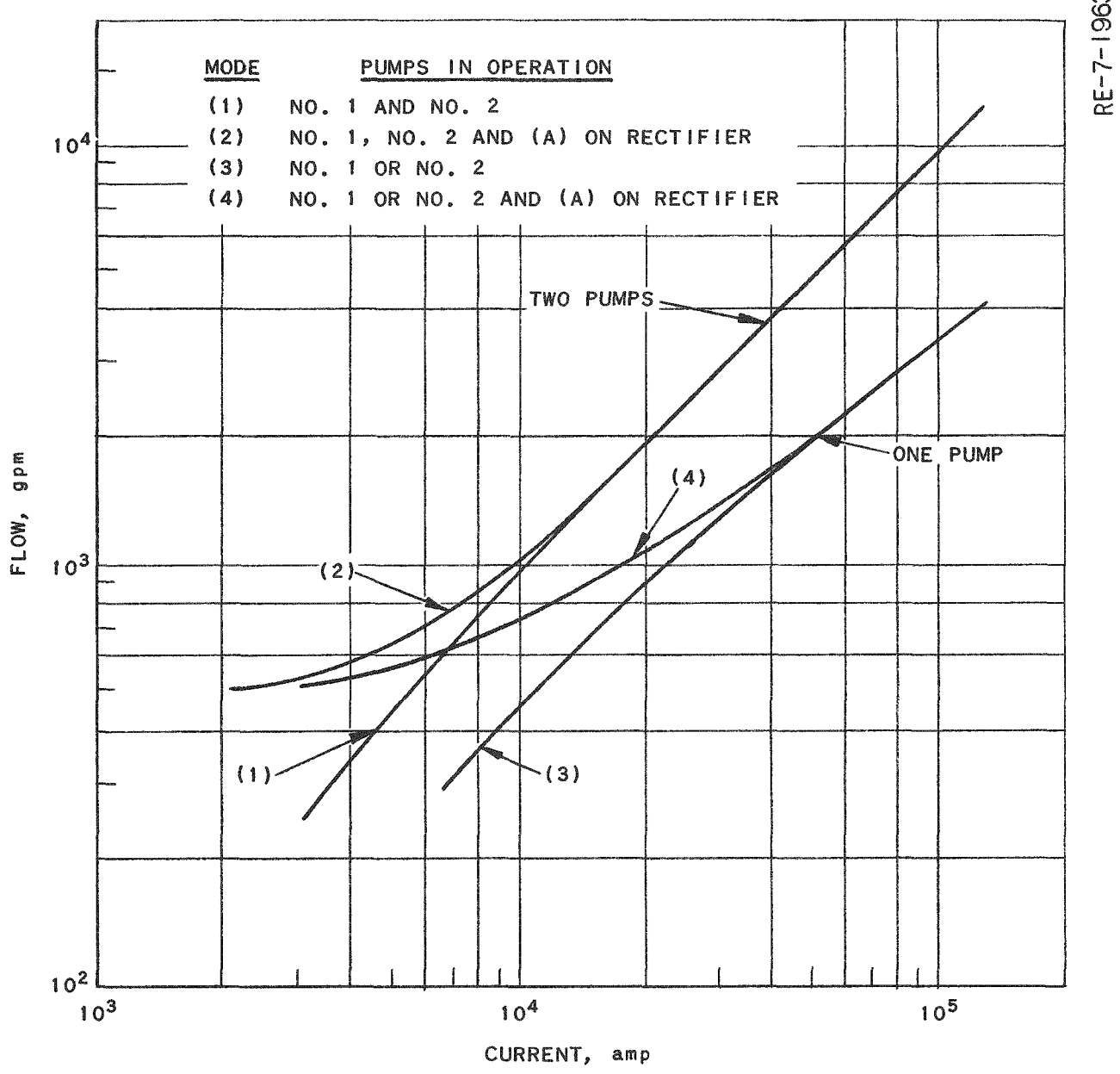

FIG. 6
FLOW RATE THROUGH REACTOR VS
MAIN PUMP RECTIFIER CURRENT

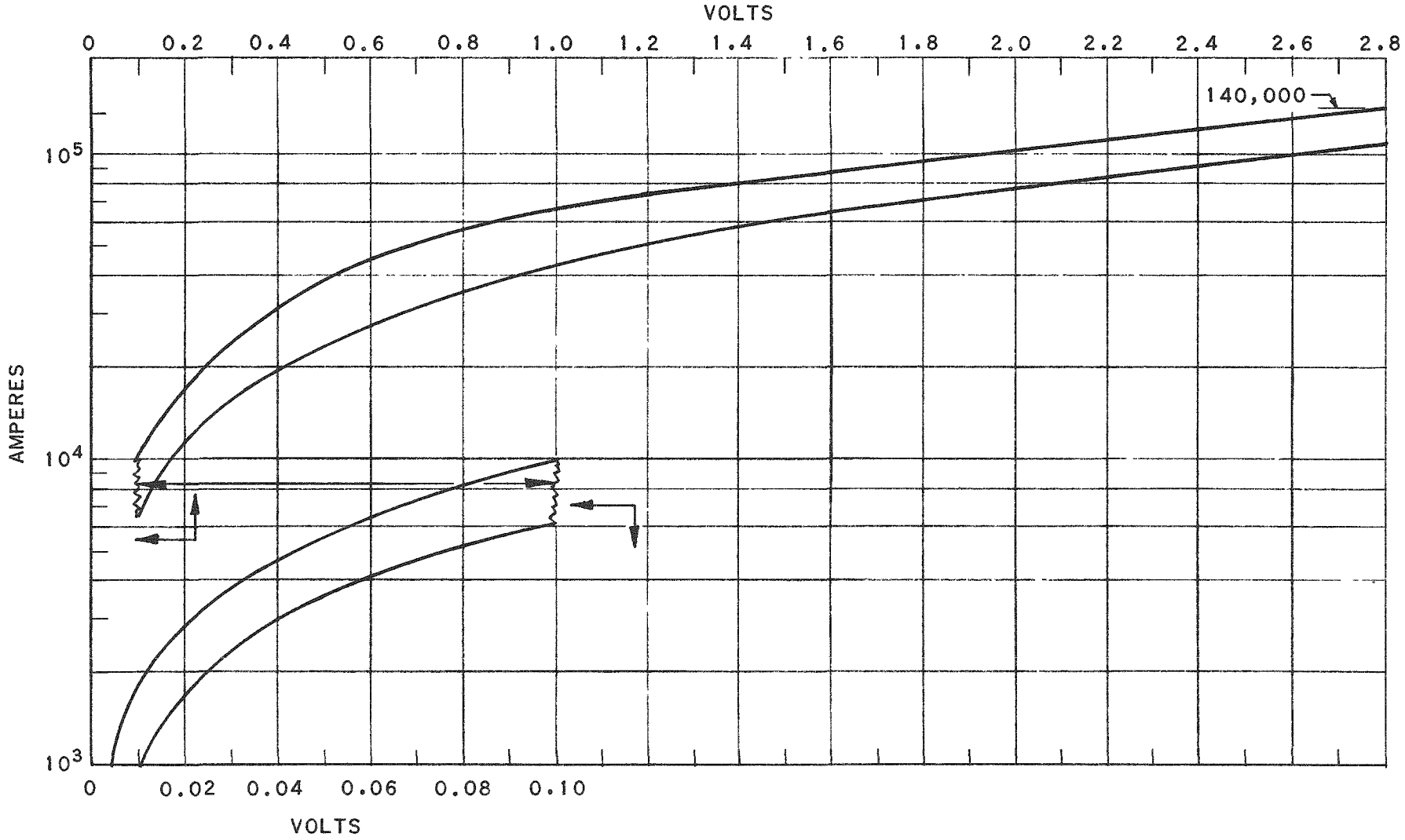

FIG. 7
MAIN PUMP RECTIFIER VOLTAGE VS CURRENT INPUT

RE-7-19640-A

RE-7-19630-A

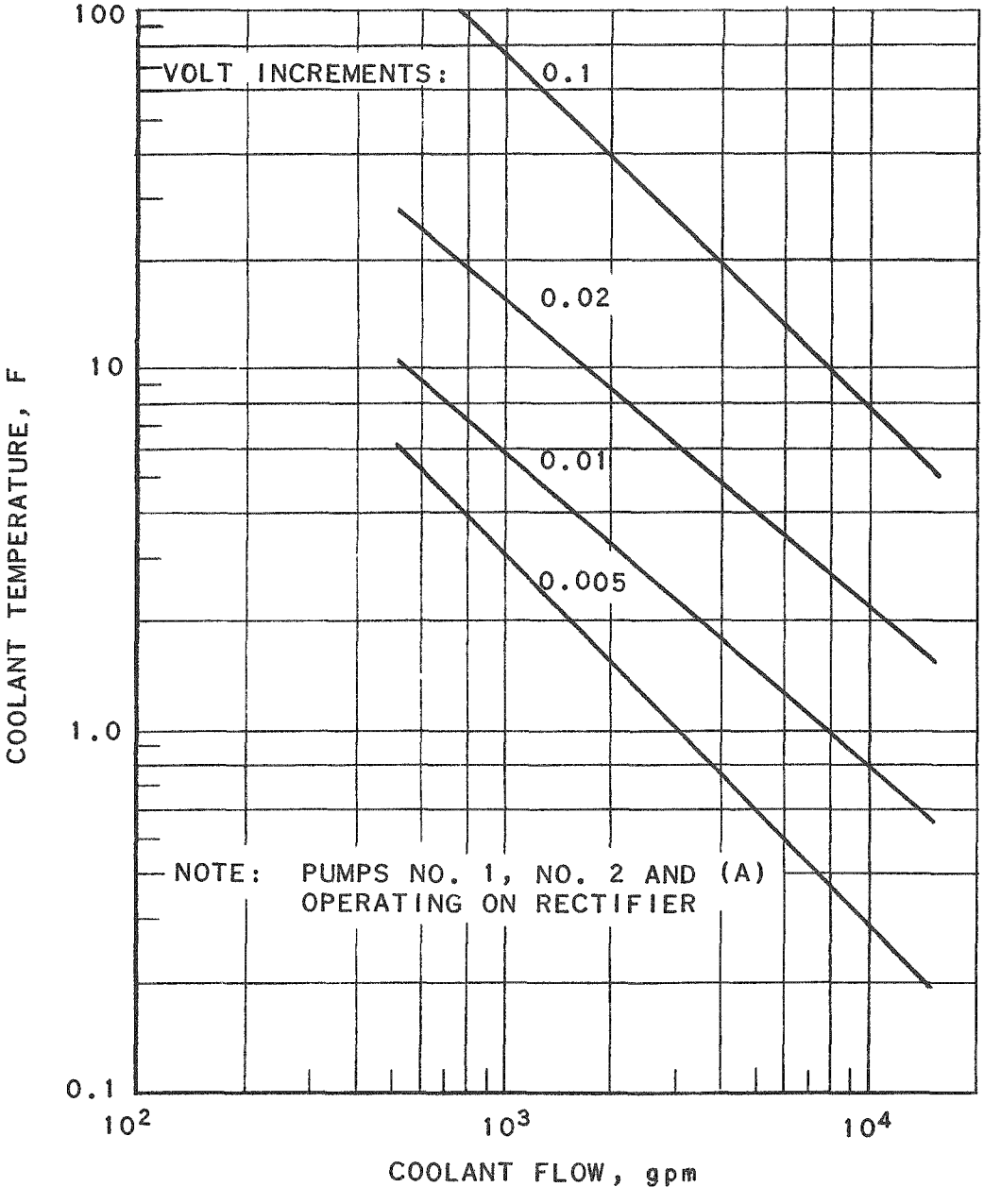

FIG. 8
EFFECT OF STEP CHANGE OF RECTIFIER VOLTAGE ON MAIN PUMP ON REACTOR COOLANT OUTLET TEMPERATURE

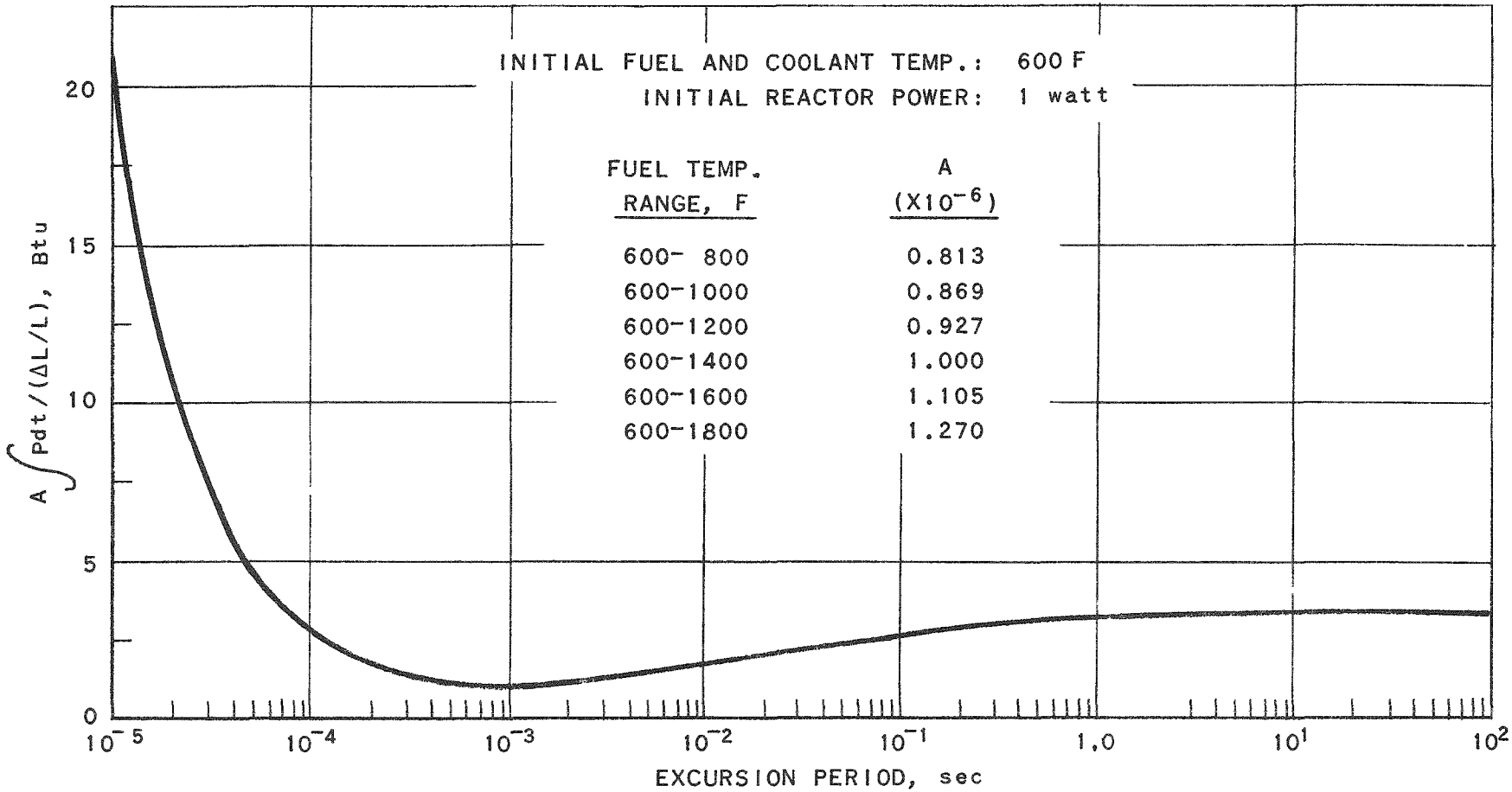

FIG. 9
RATIO OF INTEGRATED POWER TO FRACTIONAL CHANGE IN FUEL LENGTH AS A FUNCTION OF REACTOR PERIOD WITH NO COOLANT FLOW

RE-7-19639-A

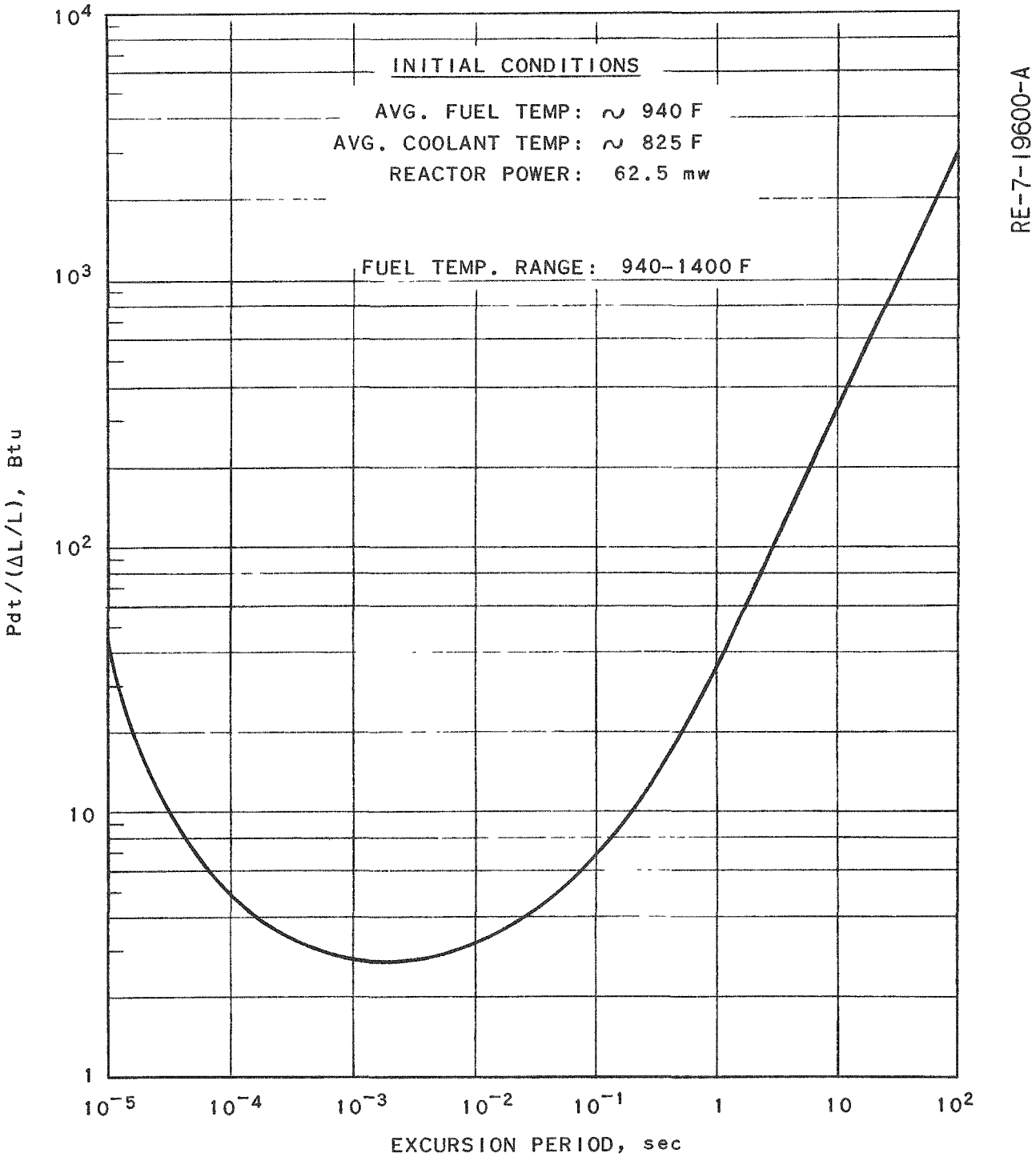

FIG. 10
RATIO OF INTEGRATED POWER TO FRACTIONAL CHANGE IN FUEL LENGTH AS A FUNCTION OF REACTOR PERIOD WITH COOLANT FLOW AT 26 fps

2. Full coolant flow: Initial average fuel and coolant temperatures the same as those anticipated for normal, full-power operation (about 940 and 825F, respectively); initial reactor power, 62.5 megawatts; excursion periods from 10^{-5} to 10^{-2} second (see Fig. 10).

Details of the study are being prepared for publication as a topical report.

C. 10,000-gpm, d-c Electromagnetic Pump, Homopolar Generator, and Test Loop - A. H. Barnes, R. A. Jaross

The present design of EBR-II provides for use of two large, direct-current, electromagnetic pumps in the primary heat transfer system. These pumps, each of about 6,000-gpm capacity at 55 psi head, operate in parallel and supply the bulk of the sodium coolant to the reactor.

A pump of the same type but of larger capacity (10,000 gpm at 50 psi head), and a homopolar generator especially designed as the power supply for the pump, have been constructed. The capacity of the present pump is considerably greater than that required in EBR-II application; it resulted from an earlier design of a primary system in which only one pump was employed.

Although expected to be capable of operation at considerably higher temperatures, the pump has a nominal temperature rating of 750F (the approximate sodium inlet temperature of the EBR-II). Because of the anticipated manner of employment in the EBR-II, it has been designed to operate completely submerged in sodium and to be readily removable from the sodium tank through a plug in the tank cover.

The homopolar generator (Fig. 11) is designed for an output of 250,000 amperes at 3 volts, a voltage somewhat in excess of that actually required for the pump. The generator, driven by a directly connected, vertically mounted, 1250-hp, 1775-rpm, induction motor, is mounted directly on top of the series-excited electromagnet of the pump so that the bus lengths are minimized. Each bus consists of a box flanged to the generator and filled with sodium which serves as a light-weight electrical conductor. The boxes are assembled to the pump terminals.

The pump and homopolar generator (with drive motor) are to be tested as a unit in a loop now under construction. The drive motor, generator, and pump will be aligned vertically in that order, from top to bottom. The pump is located in a pit 20 ft deep, with the pump suction and discharge tubes extending vertically nearly to the pit floor. The test loop connects to these tubes and runs horizontally along the pit floor. The partially completed installation is shown in Fig. 12.

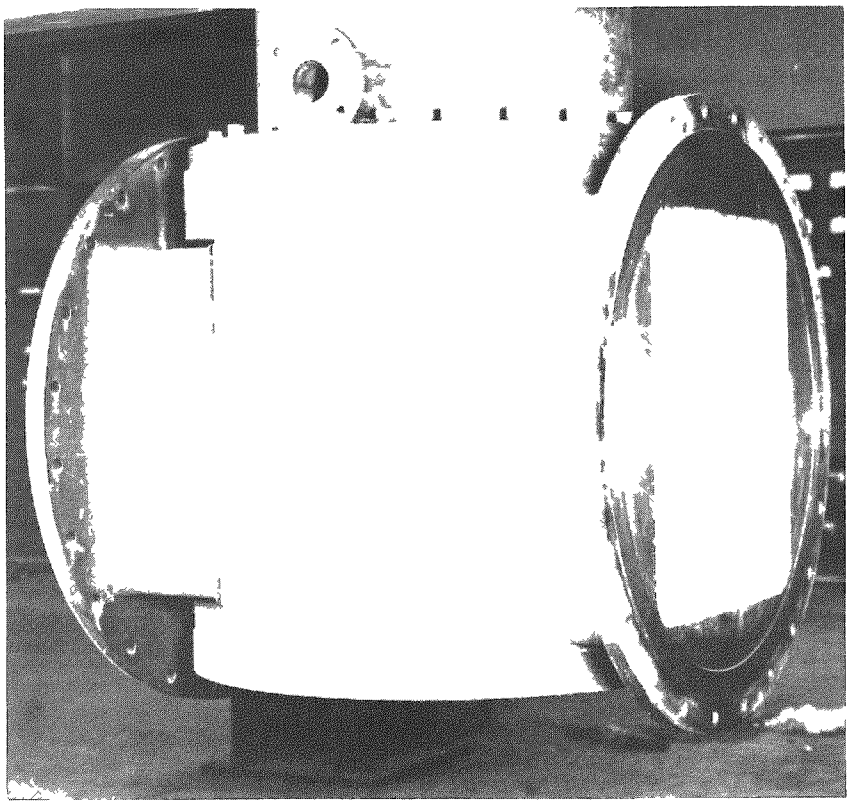

FIG. 11
HOMOPOLAR GENERATOR

D. 5,000-gpm, a-c Linear Induction Pump and Test Loop - R. A. Jaross

An alternating current, linear induction sodium pump, purchased from the General Electric Company, is to be tested for possible use in the secondary heat transfer system of EBR-II. The pump has a rated sodium temperature of 700F and is thought to be capable of pumping continuously at a somewhat higher temperature. The Class H insulated windings operate at a temperature lower than that of the sodium by virtue of a thin thermal barrier. The stator iron structure is cooled by water circulated in a continuous heavy-walled tube. The pump is rated at 5,000 gpm at 40 psi head; the electrical input to the pump is 480 volts, 755 amperes, with a 37% power factor. By using shunt capacitors for the power factor correction, the current may be reduced to 376 amperes. The operating point pump efficiency is about 41%.

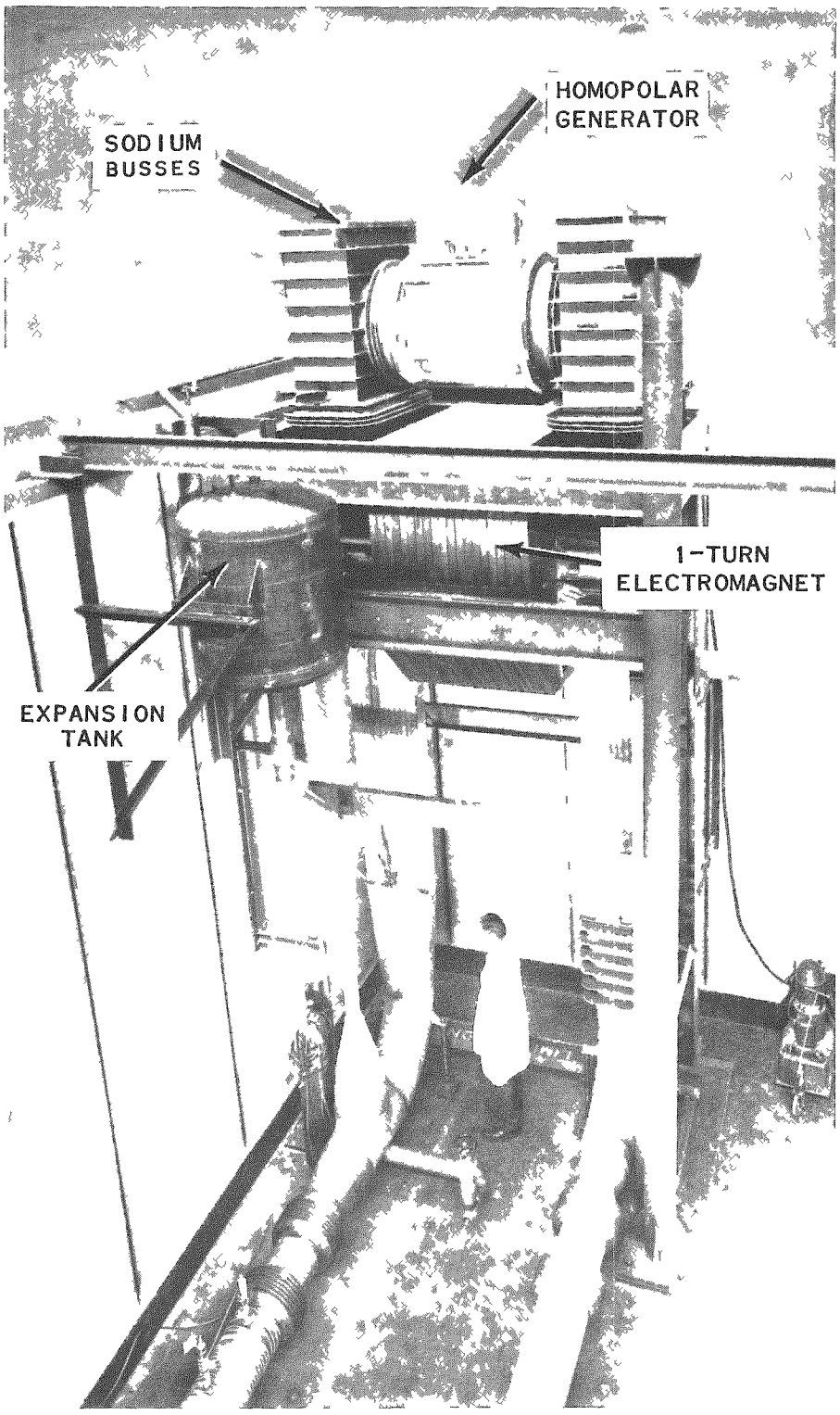

FIG. 12
d-c ELECTROMAGNETIC PUMP -
HOMOPOLAR GENERATOR TEST LOOP

This pump has many desirable features. There are no moving parts. The entire sodium enclosure is welded and is constructed of either Type 304 or 347 stainless steel. No seals are used in the primary sodium enclosure. The electrical windings and magnetic structure of the pump are located in a secondary enclosure which is filled with inert gas during operation. This secondary enclosure is sealed by a conventional metal "O" ring. In the event of a sodium leak from the primary enclosure, the secondary enclosure contains the metal and prevents leakage to the atmosphere. A sodium reaction with the cooling water would be very unlikely in this event, since a simultaneous leak in the heavy-walled water tube would be necessary. Pumping rate can be continuously and accurately controlled through control of electrical power input, thus eliminating the need for a throttling valve.

Figure 13 shows the pump installed in the test loop. The loop consists entirely of 12-inch (NPS), Schedule 10, Type 304 stainless steel pipe and fittings. A 12-inch Y-type, bellows-sealed valve will be used to accomplish the throttling required for test purposes. Since a large portion of the electrical power input to the pump must be removed from the sodium as heat, a finned air cooler is located over a 12-ft length of the loop. A built-in orifice will be used to determine the flow rate. The pump head will be indicated with pneumatic pressure transmitters.

Prior to charging the system with sodium, the temperature of the loop and pump must be increased from room temperature to approximately 250F. The pump is provided with resistance heaters for this purpose. The loop will be heated with 60-cycle induction heating. Since Type 304 stainless steel is non-magnetic, it is necessary to provide a magnetic material adjacent to the stainless steel so that the heat produced in the magnetic material can be conducted to the stainless steel pipe. This is done by cladding the entire loop with a loosely fitting, tack-welded, carbon steel skin, 3/16 in. thick. Conventional thermal insulation is then applied over this cladding (Fig. 14). After the thermal insulation is in place, a continuous coil of insulated copper wire will be wound over the entire loop. The wire will be spaced to allow approximately 30 ampere-turns per inch excitation for this size pipe.

The pump data to be obtained includes head-capacity characteristics, power input, efficiency, etc. The testing program includes continuous operation for an extended duration and a study of the characteristics of pump voltage vs flow. The results will aid in the selection of the actual pump to be used in the EBR-II secondary system.

E. 5000-gpm Mechanical Sodium Pump and Test Loop - O. S. Seim

A vertically mounted, single-stage, centrifugal pump is being considered for use in the secondary heat transfer system of the EBR-II.

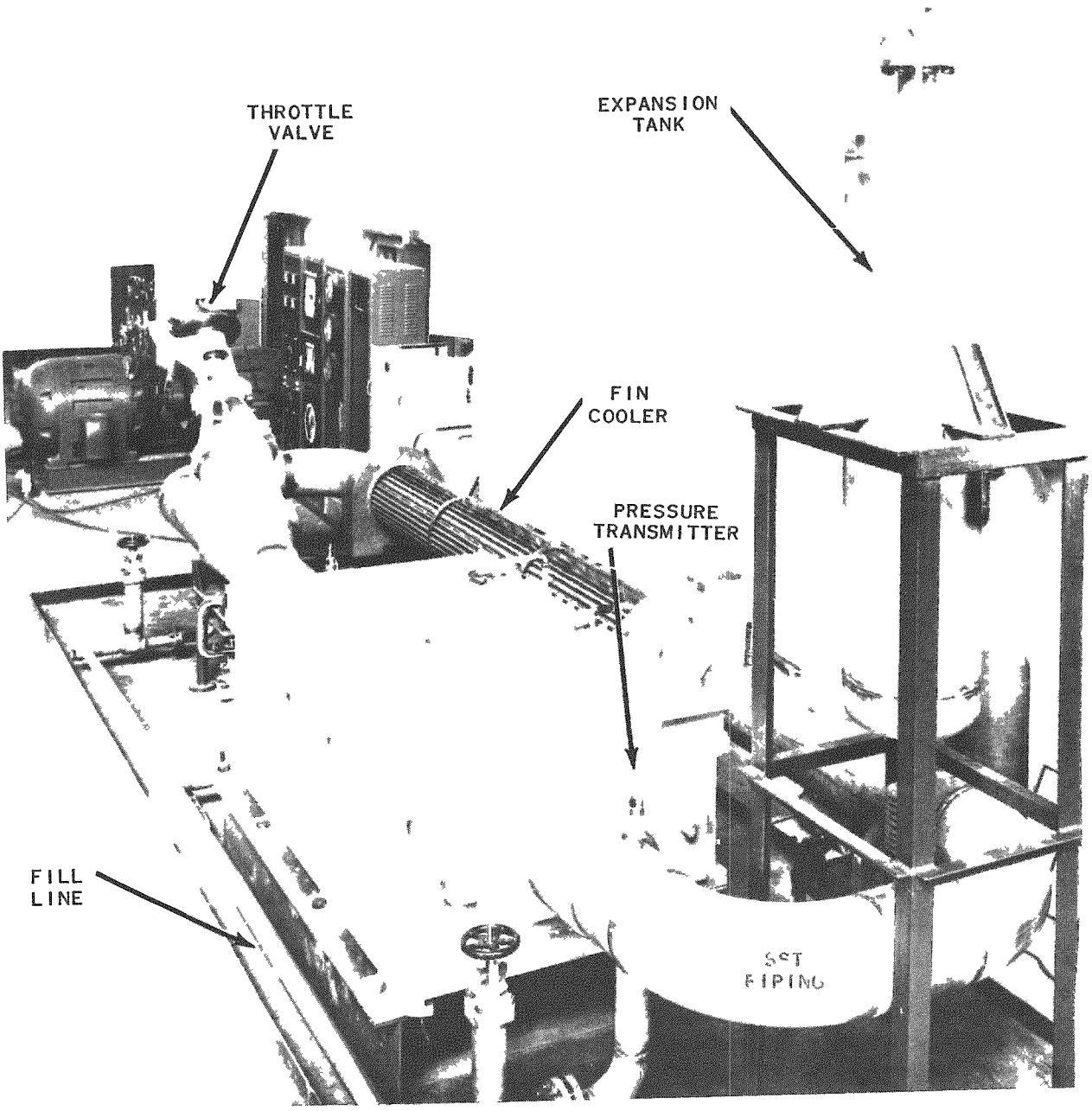

FIG. 13
5,000-gpm, a-c LINEAR INDUCTION PUMP AND TEST LOOP

26

FIG. 14
THERMAL INSULATION BEING APPLIED OVER
TACK WELDED CARBON STEEL CLADDING

The pump (Fig. 15) was constructed by the Allis-Chalmers Manufacturing Company. It is designed to circulate 5,000 gpm of sodium at a head of 40 psi and at a temperature of 700F.

The pump is driven by a standard, totally enclosed, two-speed, blower-cooled, 150-horsepower, 440-volt, a-c motor. As shown in the sectional view (Fig. 16), the pump shaft is located at the upper end by a solid coupling to the motor shaft, and at the lower end by a hydraulic (fluid piston-type) liquid metal bearing. Figure 17a shows the impeller and the large cylindrical bearing surface above it. The bearing shell (Fig. 17b) has four equally sized pockets, each of which is fed sodium from the discharge of the pump through equalizing orifices in the center of each pocket. Stellite has been applied to all bearing surfaces. To provide shaft sealing, the liquid metal is maintained at a predetermined point ($\pm$ 3 in.) above the pump discharge centerline. Baffle arrangements in this area still the sodium liquid surface. The shaft seal is of the labyrinth type employing a constant inert gas flow into the pump. The pump casing is a Type 304 stainless steel casting. The casing was inspected radiographically and with a dye-penetrant; leakage tests were conducted with a helium mass spectrometer.

A preliminary test was performed by the manufacturer, employing water as the circulating fluid. A pump efficiency of 79% was obtained at the design flow rate (Fig. 18). The bearing and other pump surfaces showed no significant wear (see Fig. 17).

A facility designed for testing of the pump is under construction. It consists of a 12-inch piping loop containing a 12-inch, Y-type, bellows-sealed, valve for flow control, augmented by equipment to control the liquid level of sodium in the pump. The piping and fittings are of Schedule 10, Type 304 stainless steel.

Figure 19 shows the present status of the facility The blower at the extreme lower left of Fig. 19 will provide heating and cooling of the system. In order to enable filling of the pump loop at approximately 250F, the blower will discharge air through steam coils into the enclosure in which the pump is mounted. The heated air then will flow through an annular area along the two horizontal pipes to an exhaust box at the 180-degree return bend end. Cooling during operation will be provided in a similar manner but with the air by-passing the steam coils. Typical high-temperature instrumentation will be employed for measurement of liquid levels, etc. Pressures will be indicated with pneumatic pressure transmitters. Both an orifice meter and an electromagnetic flow meter will be used for flow measurement. Complete head-capacity data will be obtained. In addition, a long-duration run is planned so that bearing wear and sealing efficiency can be evaluated.

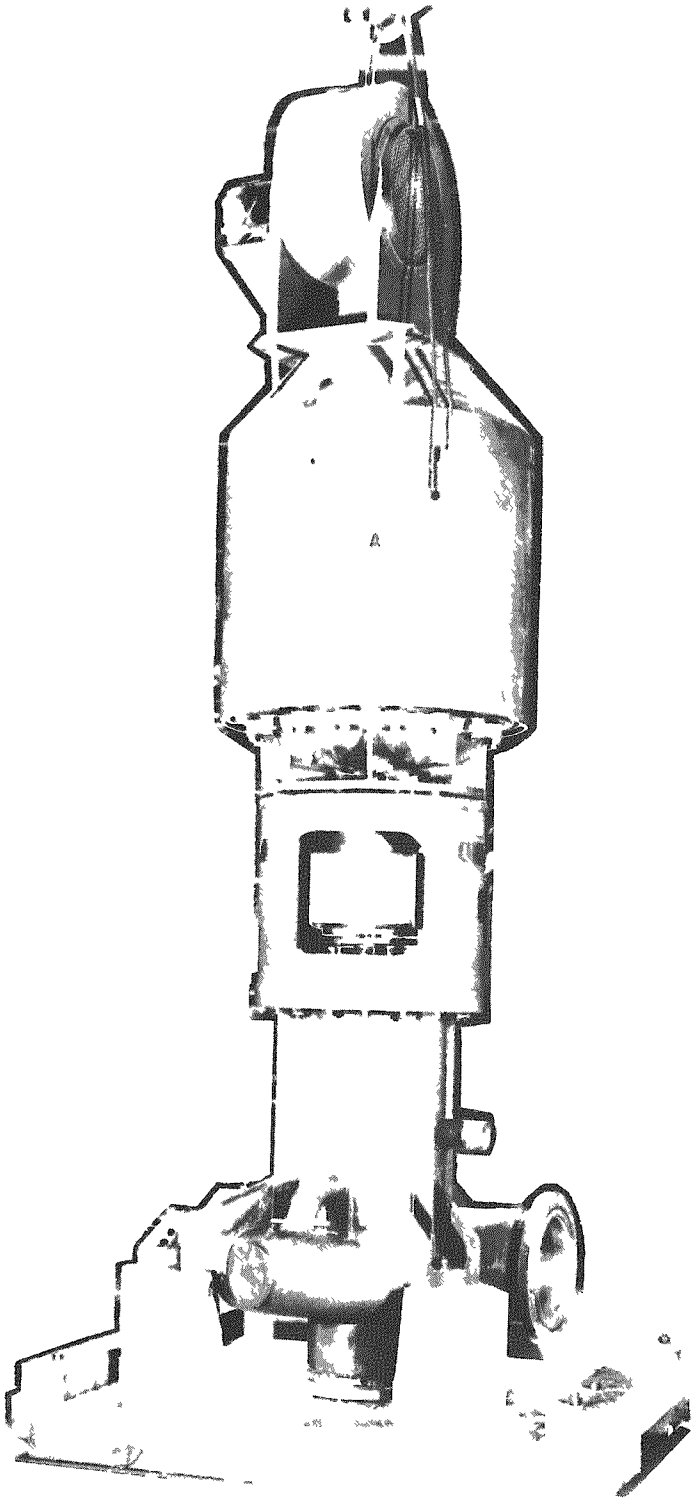

FIG. 15
5000-gpm MECHANICAL SODIUM PUMP

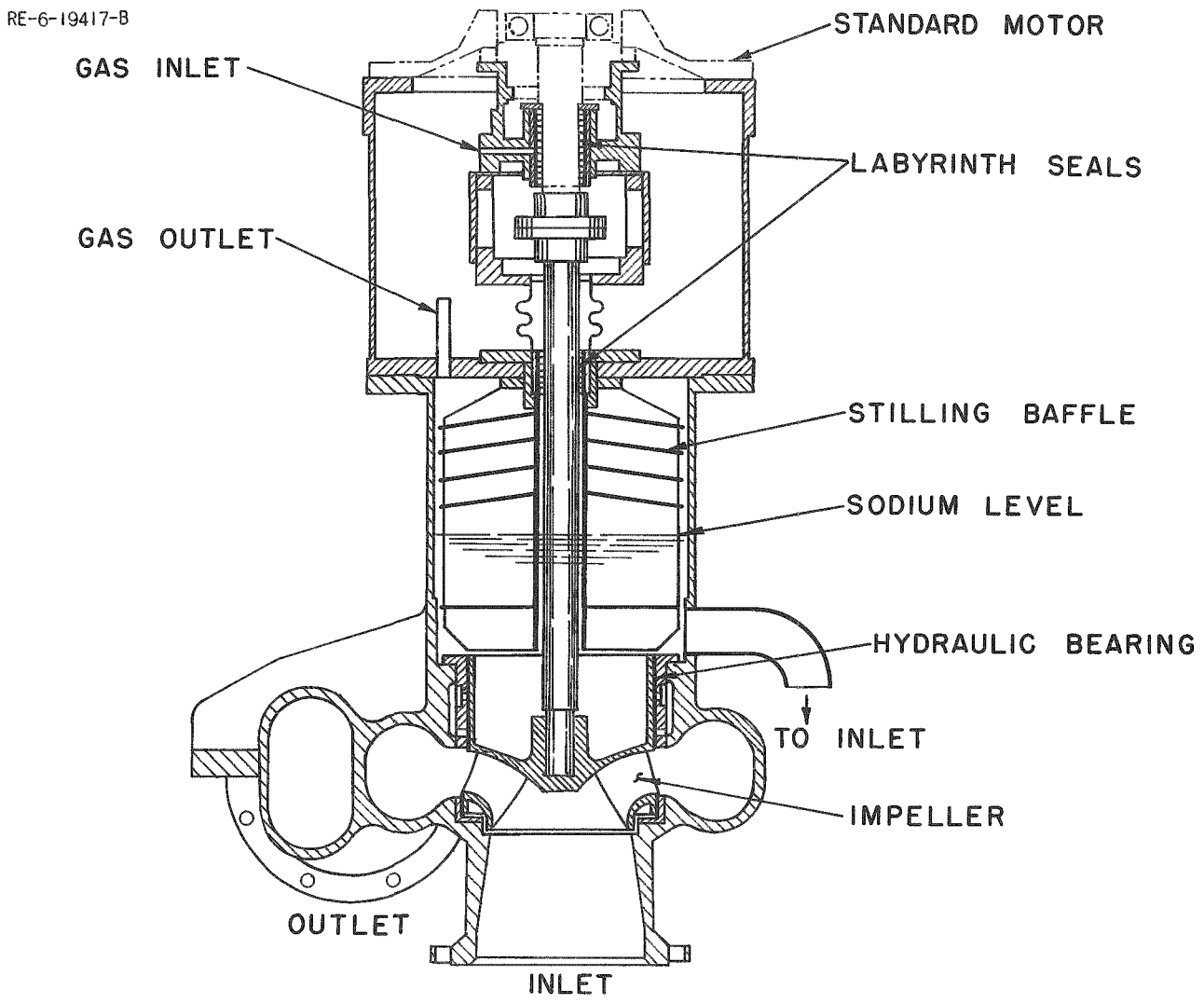

FIG. 16

SECTION OF 5000-gpm MECHANICAL PUMP

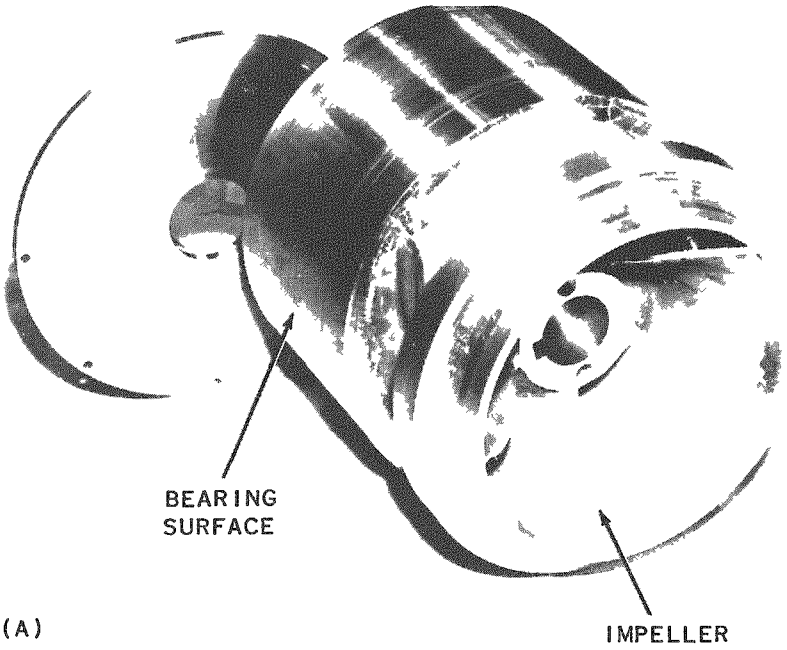

(A)

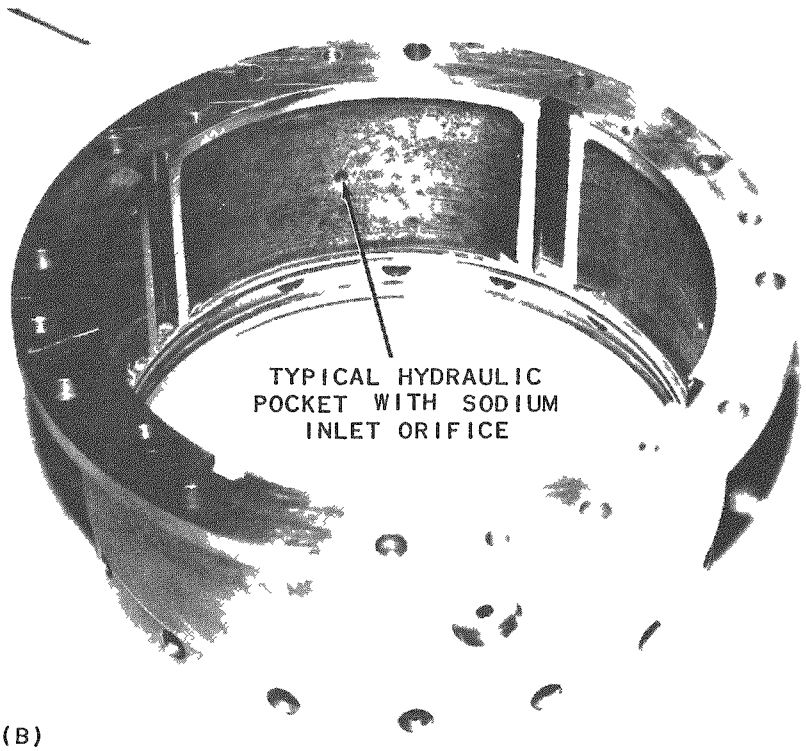

(B)

FIG. 17
APPEARANCE OF (A) PUMP IMPELLER AND SODIUM BEARING SURFACE AND (B) HYDRAULIC BEARING SHELL FOLLOWING MANUFACTURER'S TEST WITH WATER AS CIRCULATING FLUID

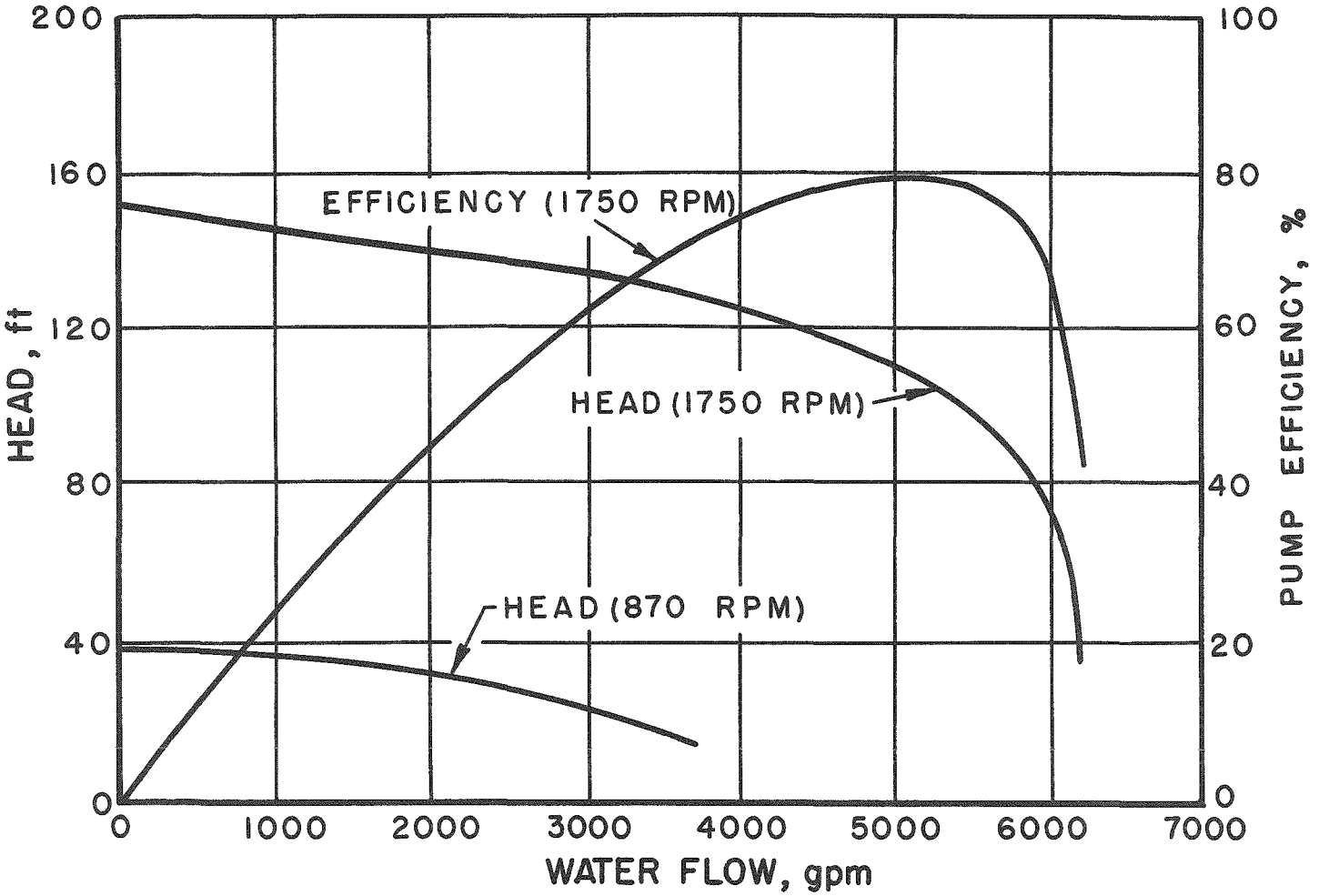

FIG. 18

PERFORMANCE CHARACTERISTICS OF 5000-gpm MECHANICAL PUMP WITH WATER AS CIRCULATING FLUID.

RE-7-19416-A

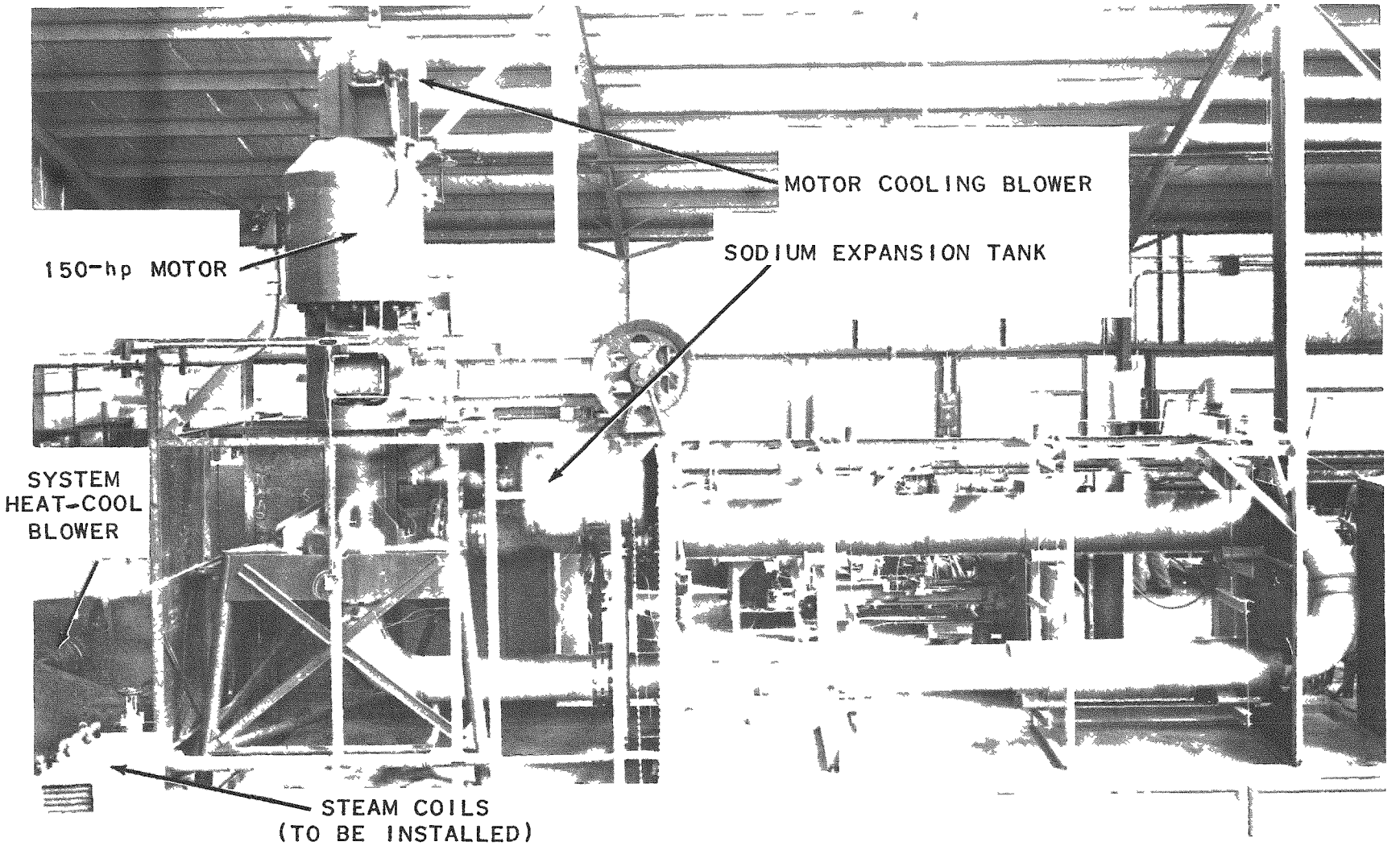

FIG. 19
5000-gpm MECHANICAL PUMP TEST LOOP

F. Rotating Plug Seal Test - A. R. Jamrog

Rotating plugs are to be employed in the primary tank cover and in the ceiling of the disassembly cell. These plugs require specially designed, meltable metal seals to prevent loss of radioactive primary tank blanket gas. These seals must be effective at all times, with the plugs in motion or at rest, and with the sealing metal in the molten or the solid condition.

A test facility (Fig. 20) has been constructed to determine the performance of a low-melting alloy, gastight seal of the present EBR-II design. The facility consists of an $8\frac{1}{2}$ ft diameter plug, ball-bearing mounted on an upper support structure, and a stationary sodium tank positioned beneath it. The sealing assembly is located at the split line between the bottom of the plug and the top of the sodium tank. The sodium tank is equipped with immersion and strip heaters to raise the sodium temperature up to 900F. Prior to testing, the free surface of the sodium will be blanketed with inert gas. The plug can be rotated at approximately 2.7 rpm by a motor-driven gear reducer.

A vertical baffle ring (skirt) of carbon steel is mounted on the underside of the rotating plug. With the plug in place above the sodium tank, this ring will be located in the center of a U-shaped, stainless steel trough mounted on the top of the tank. The trough is filled with a low-melting alloy to effect the seal.

Normally, the plug is at rest. For this condition, the sealing alloy is permitted to solidify. When plug motion is desired, the alloy is melted to permit rotation of the baffle and plug.

The melting of the sealing alloy is accomplished by 60-cycle induction heating. The major portion of the heating takes place in the carbon steel baffle, very little occurring in the stainless trough walls. The trough in which the alloy is melted has a 3-inch layer of conventional thermal insulation applied external to its outer wall. An induction coil is wound directly over this insulation, as shown schematically in Fig. 20. The coil consists of 48 turns (four layers of 12 turns each) of 2/0 gauge copper wire and has a diameter of approximately 9 ft. When excited at 468 volts, 60-cycle, the coil draws 158 amperes; power input is 35 kw, with a power factor of 0.47. This power is sufficient to raise the temperature of the alloy-filled trough from 70F to 400F in 4 hr. The maximum attainable temperature is above 600F.

Initial preparation for testing is under way.

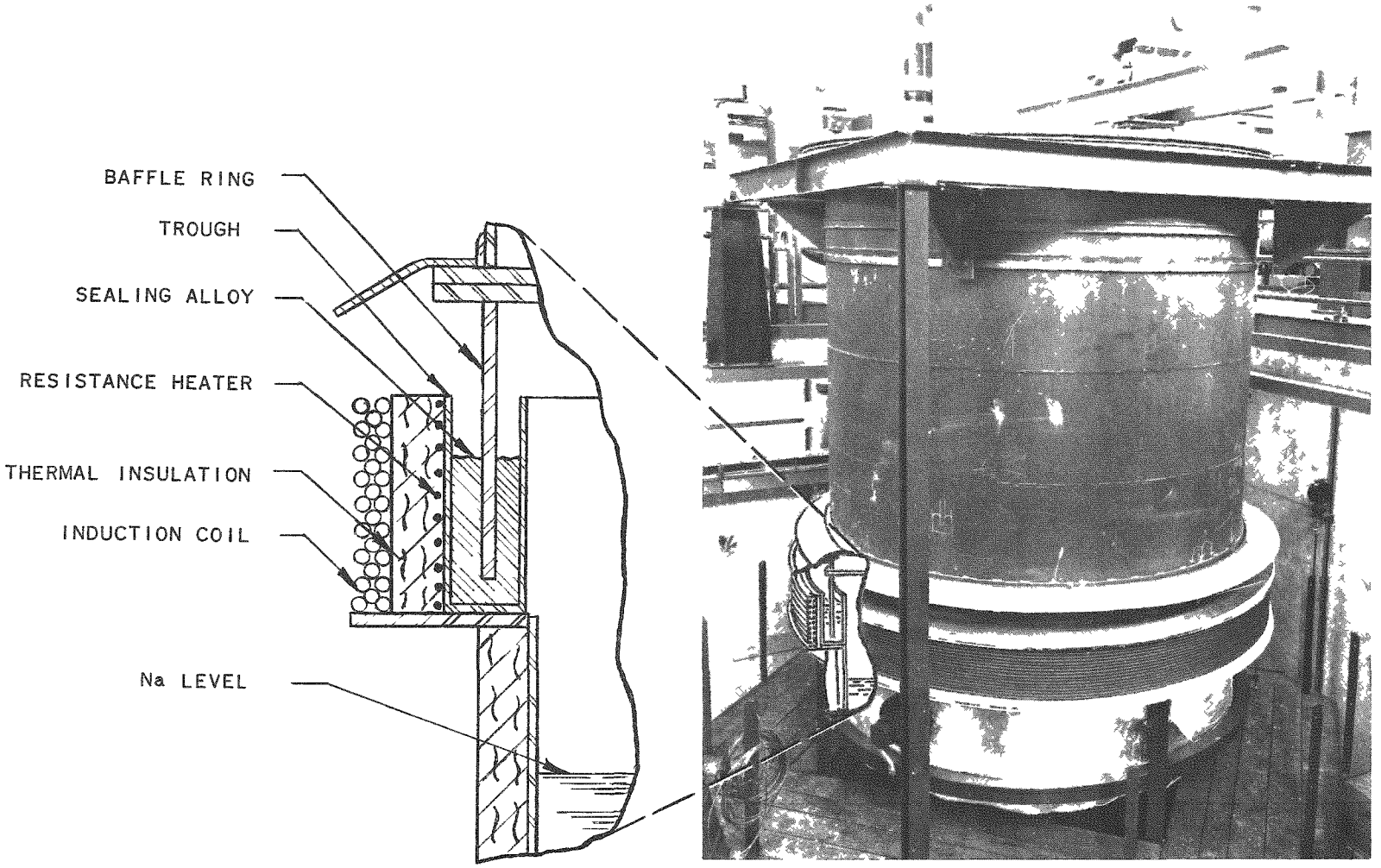

FIG. 20
ROTATING PLUG SEAL

II. SUPPORTING AND ALTERNATE DESIGN RESEARCH AND DEVELOPMENT

A. S_4 Calculations to Investigate Inhomogeneities in ZPR-III Assemblies

W. B. Loewenstein, D. Okrent

Recent experiments on critical assemblies of the EBR-II type at the ZPR-III facility indicate that appreciable reactivity effects may be observed if inhomogeneities are simply introduced into the system without varying its reference composition. These inhomogeneities are obtained by simple rearrangement, in some consistent manner, of the different plates which constitute a full drawer of the assembly.[1]

The more widely used analytical procedures for routine analyses do not directly permit the calculations of such effects in a simple fashion. However, a recently programmed solution of the S_n approximation to the transport equation does afford a method of analysis which can apply toward the prediction of reactivity effects caused by introducing inhomogeneities into the system.

The calculations are at an early stage, but up to the present time two basic areas of investigation have been considered. First, it was of interest to investigate how well one can calculate existing experiments. Here agreement between theory and experiment has been gratifying. The other topic is principally concerned with obtaining a realistic basis for the assembly of a critical system representing a PBR-type reactor.

The core volume of a PBR-type reactor is at least about five times as great as that of the EBR-II-type system which has been experimentally investigated. If the philosophy governing the assembly of EBR-II-type systems is to be followed, in terms of drawer constituents, it is apparent that an extremely large number of small pieces of constituent materials must be on hand. It would be preferable to assemble such a system with larger pieces of material in the core section than are presently used. However, this may only be done if it can be demonstrated that such an assembly retains the nuclear properties of the system which is to be investigated.

The dilute PBR core will contain fuel alloy which is 25% or less enriched, whereas for EBR-II the corresponding enrichment is about 50%. Suppose one is satisfied that, by using the enriched and depleted uranium pieces, the nuclear characteristics of EBR-II are truly obtained. Then the

---

[1] B. C. Cerutti, et al, "The Fast Critical Assembly," ANL-5513, (January, 1956).

question arises whether one can use the same fissile materials to obtain the characteristics of a core containing less enriched material. If not, the alternative is to obtain low-enrichment uranium to represent the fissile material. If one is then satisfied that the material of lower enrichment more adequately gives the nuclear parameters of interest, some choice must be made concerning the size of constituent materials in such a system.

This calulation program was instituted to obtain information concerning the topics discussed above.

1. Method of Calculation

The method of solving the transport equation by S_n approximations is described in LA-1891.[2] An S_n calculation, while still an approximation to a rigorous solution of the transport equation, should better describe the physical parameters of a chain-reacting system than a solution based on diffusion theory. This is particularly true in calculations where distances between boundaries joining different media are smaller than typical mean free paths.

Recently a program was prepared by Carlson at Los Alamos to perform S_4 calculations in slab geometry. This particular program is sufficiently versatile to permit cell calculations in slab geometry. A cell calculation, as applied to a ZPR-III assembly, would be principally concerned with the investigation of the neutron flux distribution within a given drawer of the assembly.

Suppose, then, that the space and energy-dependent flux distribution has been obtained. It should also be possible to obtain information concerning the changes in reactivity observed upon rearranging the pieces of the different materials which make up the composition of that drawer. In particular, one could hope to predict the reactivity effects associated with existing experiments. If one may reasonably calculate such observed effects, it is possible to gain confidence concerning properties of proposed assemblies based on such calculations.

It is true that a single drawer is a small part of the whole system. Therefore in order to calculate reactivity effects accurately, it is necessary to make proper assumptions concerning the neutrons leaking out

---

[2] Bengt G. Carlson, "Solution of the Transport Equation by S_n Approximations," LA-1891 (February, 1955).

of the drawer. (For simplicity, it is assumed that the central drawer is the one being calculated.) For calculations involving diffusion theory, the neutrons leaving a given volume are proportional to

$$\int_V DB^2\phi dV \quad ,$$

where

D = diffusion coefficient
B^2 = geometric buckling
ϕ = neutron flux
V = volume under consideration

This same sort of leakage condition is imposed in these particular S_4 calculations. If one is satisfied that such a term represents the neutrons leaving the drawer, it then becomes necessary to specify in what direction these neutrons are leaving the "cell." Again, simplicity has governed this decision. The calculation may be for the system illustrated, where a and b denote the boundaries.

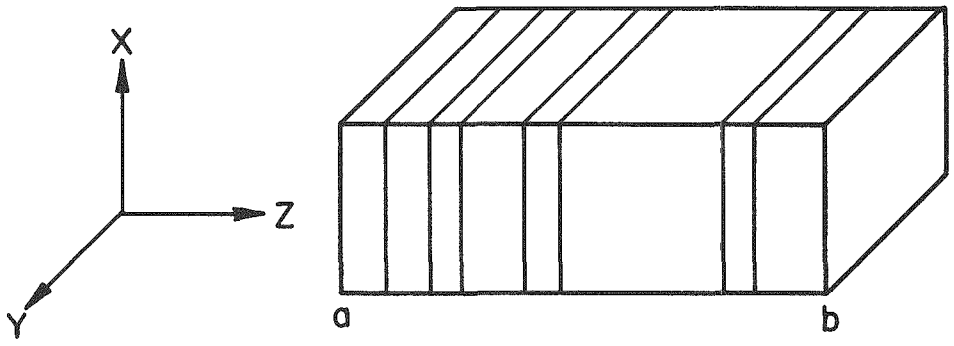

Arbitrarily, let the direction perpendicular to the slab faces be the z direction and the axes orthogonal to the z direction be the x, y axes. The calculation program is such that it is possible to specify boundary conditions at a and b for the z-dependence of the flux. However, it is not possible to explicitly specify any conditions in the x, y directions. As far as the actual calculation is concerned, the pile is assumed to be infinite in both the latter directions.

Perhaps one way to attack this problem is to require that the components of the neutron flux at a are the same as those at b, a periodic boundary condition. This would be quite realistic insofar as the calculation simulates an actual critical assembly where adjacent drawers

are, in fact, periodic. However, this did not appear to be feasible for these initial calculations. The condition applied in the calculation is the "mirror condition," which requires that the fluxes, or rather the components thereof, obey the equations $N(a+\ell) = N(a-\ell)$ and $N(b+\ell) = N(b-\ell)$. This implies that the geometrical arrangement to the "left" of a and to the "right" of b can be obtained simply by reflecting the system in the planes of a and b, respectively.

It is true that if one calculates a typical drawer of a given assembly, in general, the boundary conditions applied are not those implied by the experiments as usually performed. However, the experimental system is large and the calculation therefor by essentially isolating a single, central drawer should not be too sensitive to the particular nature of the conditions applied at the boundaries thereof. Further, it may be noted that a typical core arrangement is usually periodic and may almost obey the mirror condition. It may deviate from the latter only by the presence of a single plate, whereas the periodic condition would require a different one. Also, it is conceivable that a drawer may, to a great extent, have its components symmetrically arranged. Thus, to economize on computing time, only a segment of it need be calculated. Then the problem may well be arranged so that the "mirror condition" is preferable to the periodic condition.

The "mirror condition," as well as the periodic one, simplifies the neutron leakage considerations. It says, in effect, that there is no net neutron leakage from the drawer in the z direction. Any leakage from the system must be ascribed to neutrons leaving perpendicularly to the z direction. This leakage is then introduced in terms of a fictitious absorption cross section and changes the calculation to one associated with a system which is finite in directions perpendicular to the z axis.

The fictitious absorption cross section representing neutrons leaving the system must then be introduced into the calculation. The true absorption cross section does not appear directly in the S_n equations. Therefore, the manner of introducing the leakage is not an obvious one. One approach is to assume that one is really interested in increasing the true absorption cross section without changing the total cross section. This can be accomplished by subtracting the fictitious absorption from the elastic transport cross section, thereby implicitly increasing the time absorption term. It may also be argued that one should leave the elastic transport cross section unchanged and introduce the leakage term by adding to the total transport cross section. Both of these methods were applied to several calculations and the results compared with each other. The bulk of the analyses contained the leakage by altering the elastic transport cross section.

2. Analysis of a Calculation

The complete solution of a given system consists of a specification of the neutron flux distribution throughout the assembly as well as of its energy dependence. The angular distributions of the neutron fluxes, which are the basis of the integrated flux calculations, are also given.

Any determination of the reactivity of the system must in some manner be determined by three basic system parameters. These are the over-all rates of neutron production, absorption and leakage implicit in the calculation.

The infinite multiplication constant may be defined as the ratio of the rate of neutron production by fission to the rate of true neutron absorption, or

$$k_\infty \equiv \frac{\overline{\nu\Sigma_f}}{\overline{\Sigma_c} + \overline{\Sigma_f}} ,$$

where $\overline{\nu\Sigma_f}$, $\overline{\Sigma_c}$, and $\overline{\Sigma_f}$ are the system parameters to be evaluated. This would be the multiplication constant of the system if there were no neutron leakage. In making this calculation it must be assumed that the neutron spectrum does not change upon consideration of an infinite system, whereas the basic flux calculations may be for a finite system with leakage.

The effective multiplication factor may be defined as the ratio of the rate of neutron production to the rate of true neutron absorption plus the fictitious absorption caused by neutron leakage. This may be formulated as:

$$k_{eff} \equiv \frac{\overline{\nu\Sigma_f}}{\overline{\Sigma_c} + \overline{\Sigma_f} + \overline{L}} ,$$

where $\overline{L}$ represents the neutrons leaving the system.

Under steady-state conditions, the rate at which some particular event is taking place is simply the probability for such an event to occur multiplied by the neutron flux. For example, the rate at which neutrons are absorbed within the system is given by:

$$\int_V \int_E \Sigma_a (\underline{r},E)\, \phi (\underline{r},E)\, dE dV ,$$

where the energy is denoted by E and the volume by V. Thus the average parameters which enter into the expressions for reactivity are as follows:

$$\overline{\Sigma}_a = \frac{\int_V \int_E \Sigma_a (\underline{r},E)\ \phi(\underline{r},E)\ dEdV}{\int_V \int_E \phi(\underline{r},E)\ dEdV}$$

3. Experiments to be Analyzed

Assemblies 2 and 2C are typical EBR-II type criticals whose over-all core and blanket compositions are reported in ANL-5513.[1] The core is essentially cylindrical with a height of about 41 cm and an L/D of about unity. The typical drawer loading of Assemblies 2 and 2C (see Fig. 3 of ANL-5513) is shown in Fig. 21. Assembly 2 represents as homogeneous a system as can be accomplished with constituent plates of 1/8 in. thickness. Assembly 2C is one where all of the enriched and depleted material is "bunched" in the center of the drawer. It was experimentally determined that upon such a rearrangement, with the over-all drawer composition unchanged, that the critical mass of Assembly 2C was 9.2 kg less than that associated with Assembly 2.

Assemblies 2A and 2E are similar to 2 and 2C except that all the depleted uranium was removed from the core and replaced by stainless steel plates. Fig. 21 also gives typical drawer loadings for these assemblies. Again it can be seen that Assembly 2A is a more homogeneous type of loading than that associated with Assembly 2E. The critical mass of Assembly 2E was found to be 9.9 kg less than that of Assembly 2A.

4. Completed Calculations

A series of calculations pertaining to ZPR-III assemblies, both completed and proposed, have been analyzed for certain properties. It is to be noted, also, that the edges of the drawers are not necessarily considered as cell boundaries for the calculations. Problems 3 and 8 as well as 9 and 10 differed only in the manner in which the leakage term was introduced into the calculation. Problem 12 was completed with no leakage term; hence it represents the calculation of an infinite system.

Initially, one would like to compare the calculated flux distribution with one experimentally measured. However, such information has only been obtained through the integrated fission rate measurements.[3]

---

[3]Private communication, F. Kirn, NRTS, Idaho Falls, Idaho.

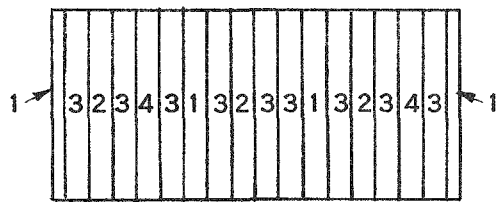

ASSEMBLY 2
PROBLEMS 3, 8, 12

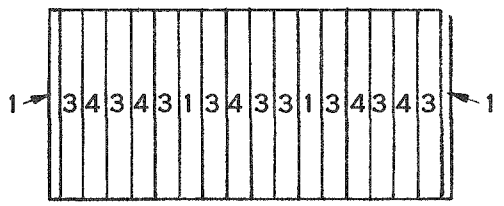

ASSEMBLY 2A
PROBLEM 13

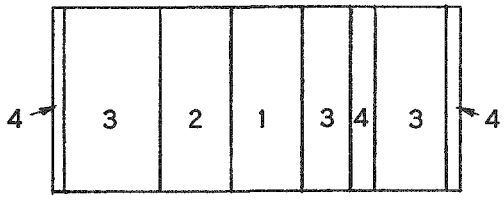

ASSEMBLY 2C
PROBLEMS 9, 10

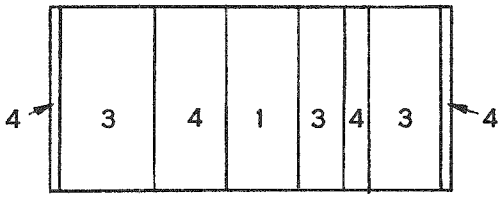

ASSEMBLY 2E
PROBLEM 14

MATERIAL IDENTIFICATION

1	ENRICHED URANIUM	(E)
2	DEPLETED URANIUM	(U)
3	61% ALUMINUM	(.61 Al)
4	IRON	(Fe)

RE-8-19566-A

FIG. 21
SCHEMATICS OF DRAWER LOADINGS

Fig. 22 shows the variations in the rates of U^{235} and U^{238} fissions across a drawer in Assembly 2C. Problems 9 and 10 are the basis for the calculation. The experimental rates were normalized to those calculated at one point. Similarly, Fig. 23 shows a comparison between fission rates based on problems 3 and 8 and the fragmentary information obtained on Assembly 2.

It should be noted that the experimental rates are obtained by essentially perturbing the system by the introduction of the foils to be activated. This could have an effect on the flux distribution, especially in plates not otherwise containing fissionable material. Hence, exact agreement between calculation and experiment is not expected. However, Figs. 22 and 23 indicate, at least, qualitative agreement between theory and experiments.

One would like to compare the reactivity effects observed in changing Assembly 2 and 2C and 2A to 2E. To facilitate this interpretation Table I has been compiled. The one-group parameters associated with each problem are listed as well as the two types of calculated multiplication constants discussed previously. (The one-group parameters were, in effect, calculated by hand and, in order to reduce chance for error, were checked in many cases by different numerical integration schemes.)

5. Analysis of Problems Related to Assemblies 2 and 2C

Experimentally, the critical masses of Assemblies 2 and 2C are 136.0 and 126.8 kg of U^{235}, respectively, indicating a difference of 9.2 kg between the two loadings. It must be considered that the loading was changed by changing the core radius, i.e., removing fuel from the edge of the core. Experimentally, the worth of core material at the edge appears to be 84 inhours per kilogram, indicating that $\frac{\delta k}{\delta M} \sim 0.0021$, and indicating further that $\frac{\delta k}{k} \sim 0.28 \ \frac{\delta M}{M}$. (This latter relationship is very much like the frequently used relationship

$$\frac{\delta k}{k} \sim 0.25 \ \frac{\delta M}{M}$$

when fuel is added near the core edge; it is based on theoretical considerations.) A difference of 9.2 kg in the critical mass would indicate that a reactivity change of 1.93% was observed. Calculated effects depend on particular solutions as well as methods of calculation. Using the parameter k_{eff} as a basis, the calculated effects were such that

$$\text{average } \delta k_{eff} = 1.82\% \quad .$$

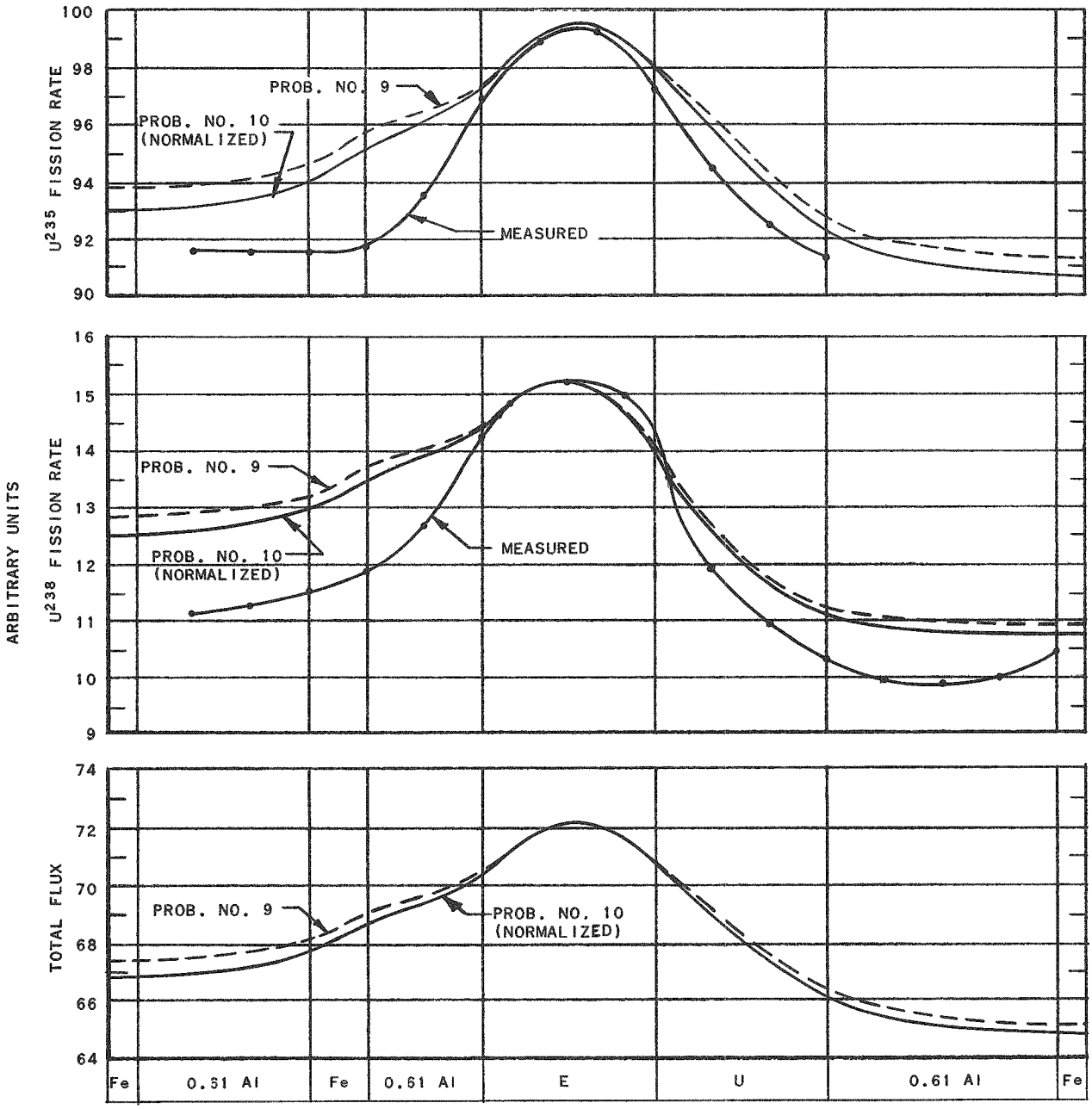

RE-7-19637-B

FIG. 22
COMPARISON OF MEASURED WITH CALCULATED FISSION RATES
(PROBLEMS NO. 9 AND NO. 10)

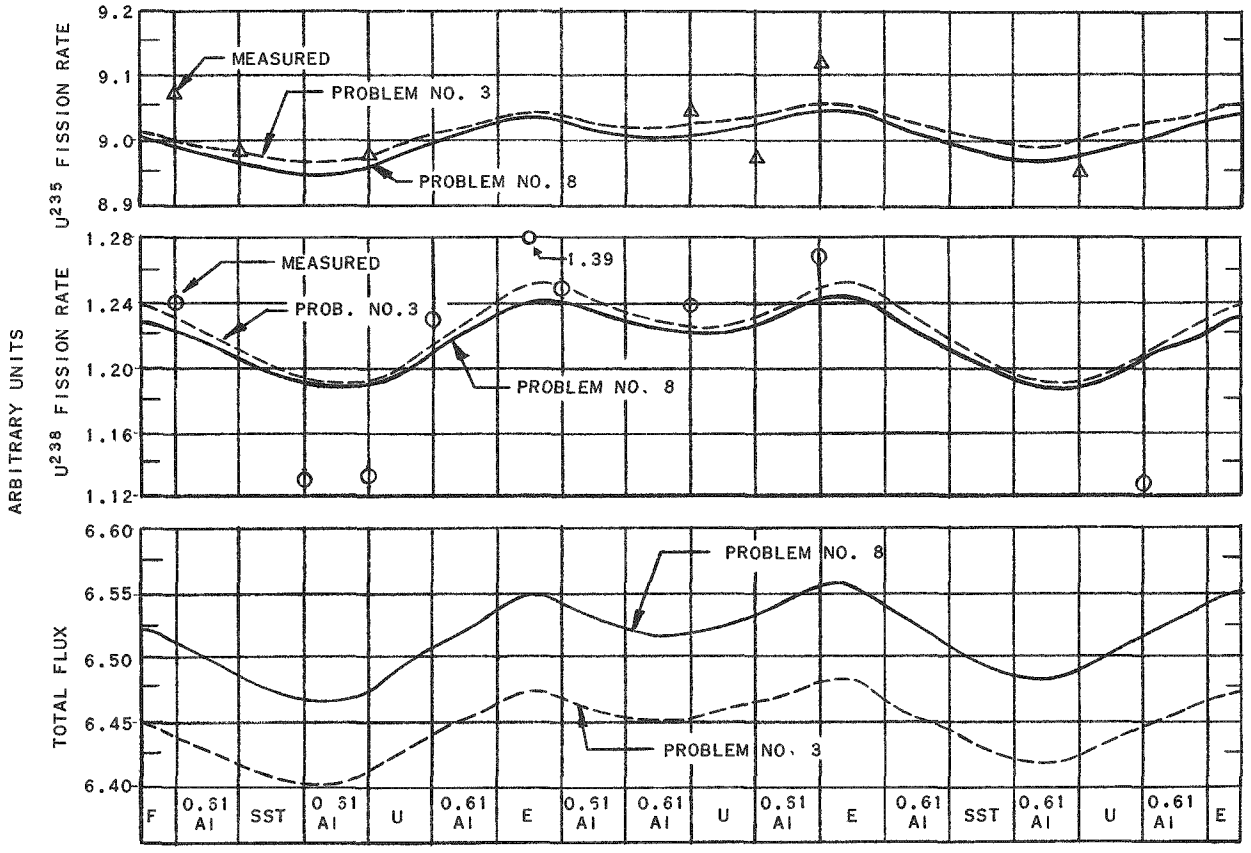

RE-7-19644-B

FIG. 23
COMPARISON OF MEASURED WITH CALCULATED FISSION RATES
(PROBLEMS NO. 3 AND NO. 8)

Table I

SUMMARY OF CALCULATED PARAMETERS FOR S_4 ANALYSIS

Problem	Assembly	Calc. Method	$\iint \phi dEdV$	$\overline{\Sigma_c}$	$\overline{\Sigma_f}$	$\overline{\nu\Sigma_f}$	$\overline{L}$	k_∞	k_{eff}
3	2	1	34.78	0.00296	0.01171	0.03004	0.01525	2.04751	1.00374
3		2	34.78	0.00296	0.01171	0.03004	0.01525	2.04759	1.00387
8	2	1	35.15	0.00286	0.01156	0.02968	0.01535	2.05757	0.99638
8		2	35.16	0.00286	0.01158	0.02972	0.01535	2.05747	0.99752
9	2C	1	367.67	0.00295	0.01205	0.03099	0.01532	2.06497	1.02192
9		2	367.66	0.00295	0.01204	0.03096	0.01529	2.06507	1.02270
10	2C	1	33.83	0.00287	0.01202	0.03093	0.01534	2.07694	1.02317
10		2	33.89	0.00289	0.01201	0.03088	0.01537	2.07351	1.02061
12	2	2	35.27	0.00263	0.01147	0.02958		2.09756	0.98883
13	2A	1	35.40	0.00174	0.01051	0.02694	0.01475	2.19963	0.99805
13		2	35.40	0.00174	0.01051	0.02695	0.01475	2.19972	0.99820
14	2E	1	34.53	0.00172	0.01082	0.02782	0.01483	2.21816	1.01636
14		2	34.53	0.00172	0.01082	0.02782	0.01483	2.21830	1.01659
15	PBR	1	255.5	0.00400	0.00639	0.01624	0.00581	1.56327	1.00262
15		2	255.5	0.00400	0.00639	0.01625	0.00581	1.56342	1.00277
16	PBR	1	11.67	0.00395	0.00641	0.01632	0.00583	1.57426	1.00730
16		2	11.67	0.00395	0.00641	0.01632	0.00583	1.57434	1.00739
17	PBR	1	50.25	0.00372	0.00624	0.01590	0.00596	1.59605	0.99867
17		2	50.25	0.00371	0.00624	0.01590	0.00596	1.59629	0.99883
18	PBR	1	50.18	0.00373	0.00623	0.01586	0.00595	1.59227	0.99679
18		2	50.18	0.00373	0.00623	0.01586	0.00595	1.59280	0.99697

This calculation was based on problems 3 and 9. The same effect may be calculated on the basis of Problems 8 and 10; this gave:

$$\text{average } \delta k_{eff} = 2.25\% \quad .$$

If it is assumed that the experimental calibration is reliable, then a detailed analysis of Table I will show that the leakage conditions imposed in Problems 3 and 9 are preferable to those of Problems 8 and 10.

6. Analysis of Problems Related to Assemblies 2A and 2E

Experimentally, the critical masses of Assemblies 2A and 2E are 147.7 and 137.8 kg of U^{235}, respectively, indicating a difference of 9.9 kg. To obtain the latter estimate of critical mass, the worth of fuel near the core edge was assumed from the calibration in connection with Assembly 2. Therefore, using the relationship established in the previous section:

$$\frac{\delta k}{\delta M} \sim 0.0021 \quad ,$$

the observed reactivity change associated in going from Assembly 2A to 2E was estimated to be 2.08%. The calculated effect on the basis of the parameter k_{eff} was:

$$\text{average } \delta k_{eff} = 1.83\% \quad .$$

Figs. 24 and 25 give spectral information on these assemblies.

7. Analysis of Problems Related to The PBR Critical

An assembly with a core larger than that of an EBR-II type of system will have a considerably lower enrichment in the fuel alloy. Whereas the U^{235}/U^{238} enrichment ratio for an EBR-II system is about one, a system similar to the PBR Critical will have a U^{235}/U^{238} ratio of about 1:4. The problems shown in Fig. 26 are all in the latter category. The homogenized composition of each of these problems is the same. The purposes here were to study the effects of different arrangements using fuel and diluent plates presently available, as well as to consider the possibility of using fuel plates of considerably lower enrichment than those now on hand at the ZPR-III facility.

Problem 15 is a typical drawer arrangement if one were to build a low-enrichment assembly with the philosophy governing the construction of the more enriched EBR-II-type assemblies.

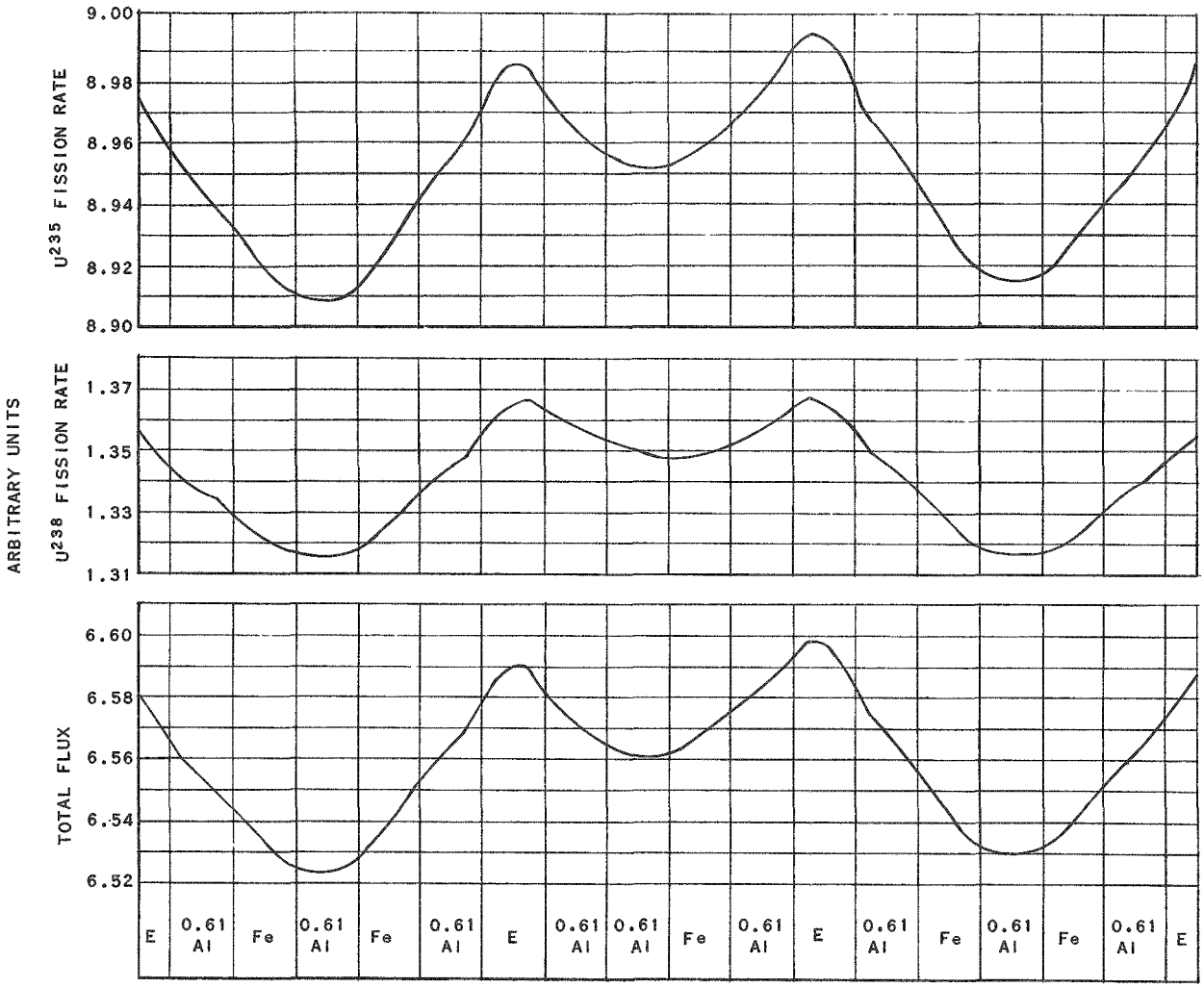

RE-7-19643-B

FIG. 24
SPATIAL DISTRIBUTION OF FISSION RATES AND TOTAL FLUX IN ASSEMBLY 2A

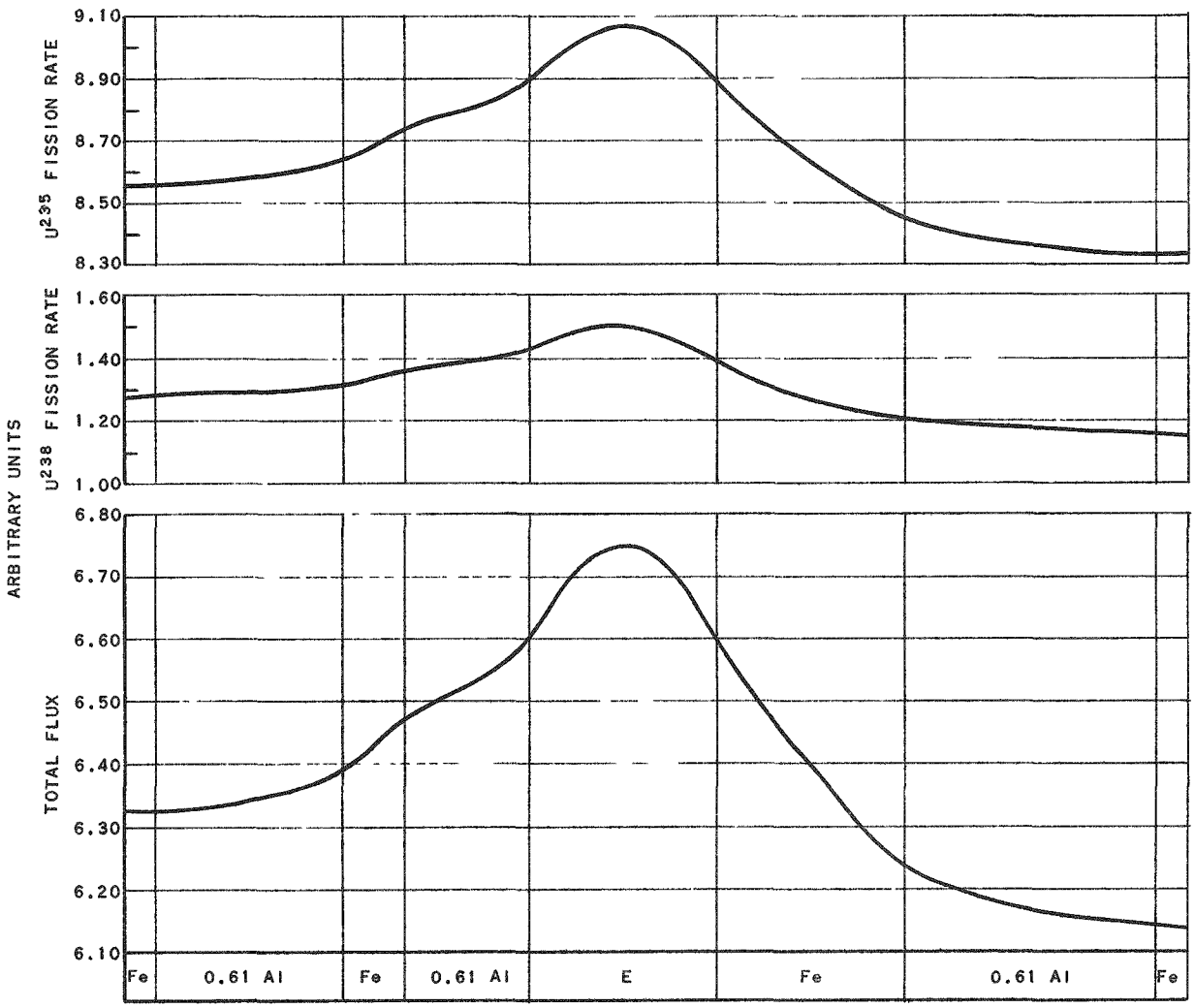

FIG. 25
SPATIAL DISTRIBUTION OF FISSION RATES
AND TOTAL FLUX IN ASSEMBLY 2E

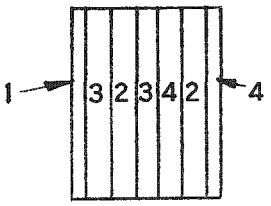

PROBLEM 15

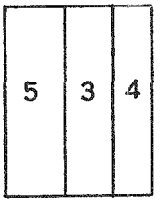

PROBLEM 17

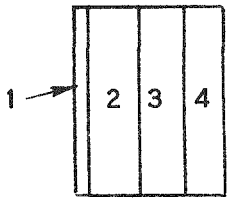

PROBLEM 16

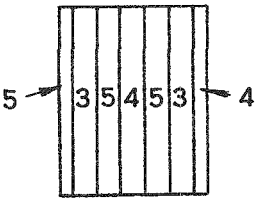

PROBLEM 18

MATERIAL IDENTIFICATION

1	ENRICHED URANIUM	(E)
2	DEPLETED URANIUM	(U)
3	61% ALUMINUM	(.61 Al)
4	IRON	(Fe)
5	PARTIALLY ENRICHED URANIUM	(P)

FIG. 26
SCHEMATICS OF DRAWER LOADINGS
FOR PROPOSED CRITICAL ASSEMBLIES

Problem 16 is an arrangement which might also be assembled with existing constituents but would provide for easier assembly because of fewer pieces.

Problem 18 represents, perhaps, the most homogeneous arrangement to be obtained using the partially enriched uranium, provided no plates of less than 1/8-in. thickness are to be used.

Problem 17 represents a system using the partially enriched uranium but which, for simplicity, is constructed with thicker plates.

Initially, Problems 15 and 16 were compared. This is to investigate the "bunching" of fissile material when the system is assembled with both fully enriched and depleted plates. The calculated reactivity change was:

$$\delta k_{eff}\ (15 \rightarrow 16) = +\ 0.47\% \quad .$$

Similarly, one can compare Problem 17 with 18 to determine the "bunching" effect when the system is based on the assembly of partially enriched uranium plates. This reactivity effect was calculated as:

$$\delta k_{eff}\ (18 \rightarrow 17) = +\ 0.19\% \quad .$$

Comparison of Problem 15 with 18 is useful. This indicates what kind of reactivity change would be observed if the most homogeneous arrangement is constructed with fully enriched and depleted plates and then later assembled with partially enriched plates. This was calculated to be:

$$\delta k_{eff}\ (18 \rightarrow 15) = +\ 0.58\% \quad .$$

It appeared that the most reactive configuration is that associated with Problem 16, the "bunched" assembly using fully enriched and fully depleted plates. The least reactive was that associated with Problem 18, the latter being the most homogeneous array for this series of calculations. It was also the one most closely approximating the actual reactor under consideration.

Figs. 27 to 30 give spectral information on these problems.

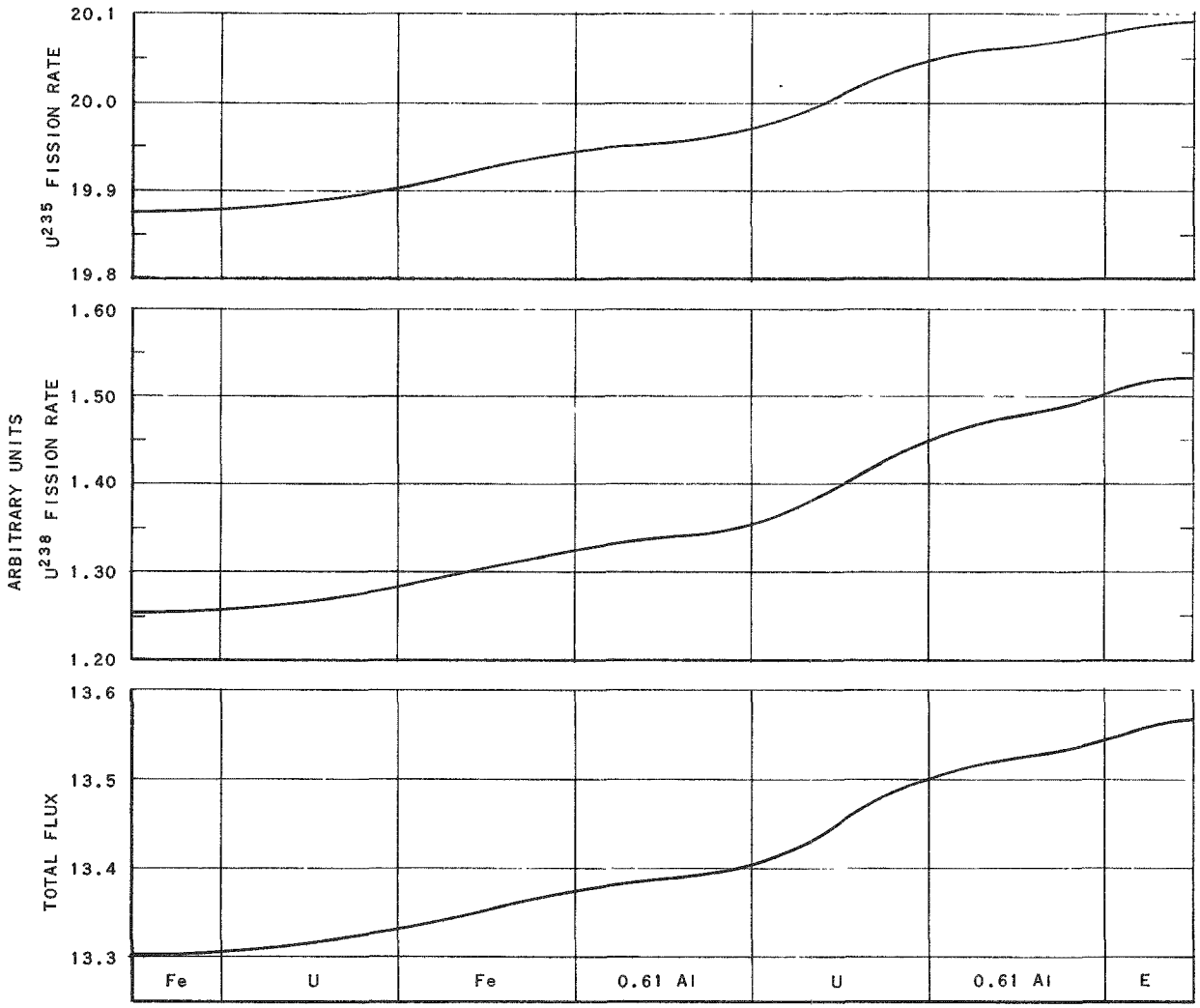

RE-7-19642-B

FIG. 27
SPATIAL DISTRIBUTION OF FISSION RATES AND TOTAL FLUX
(PBR ANALYSIS: PROBLEM NO. 15)

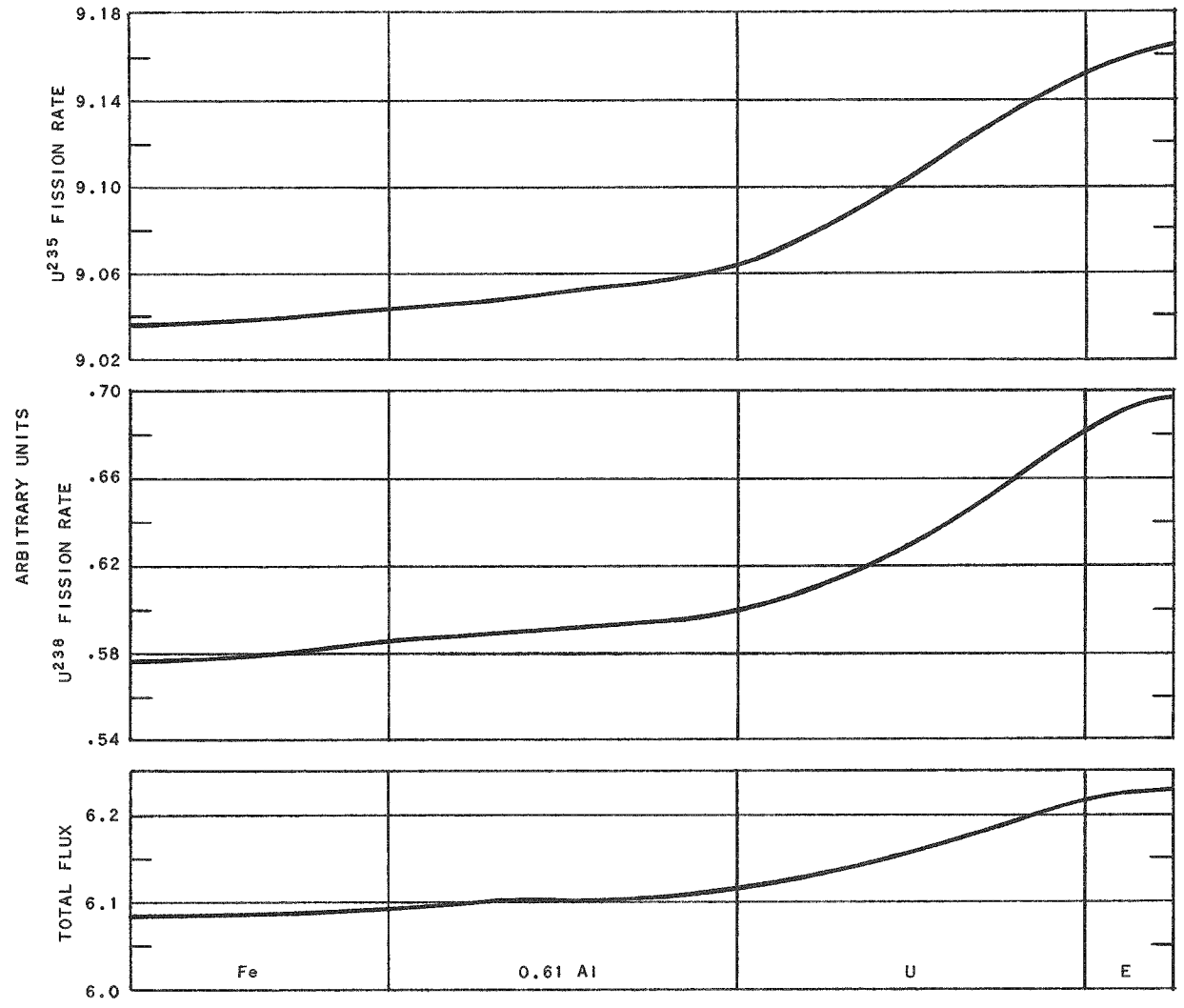

FIG. 28
SPATIAL DISTRIBUTION OF FISSION RATES AND TOTAL FLUX
(PBR ANALYSIS: PROBLEM NO. 16)

RE-7-19635-B

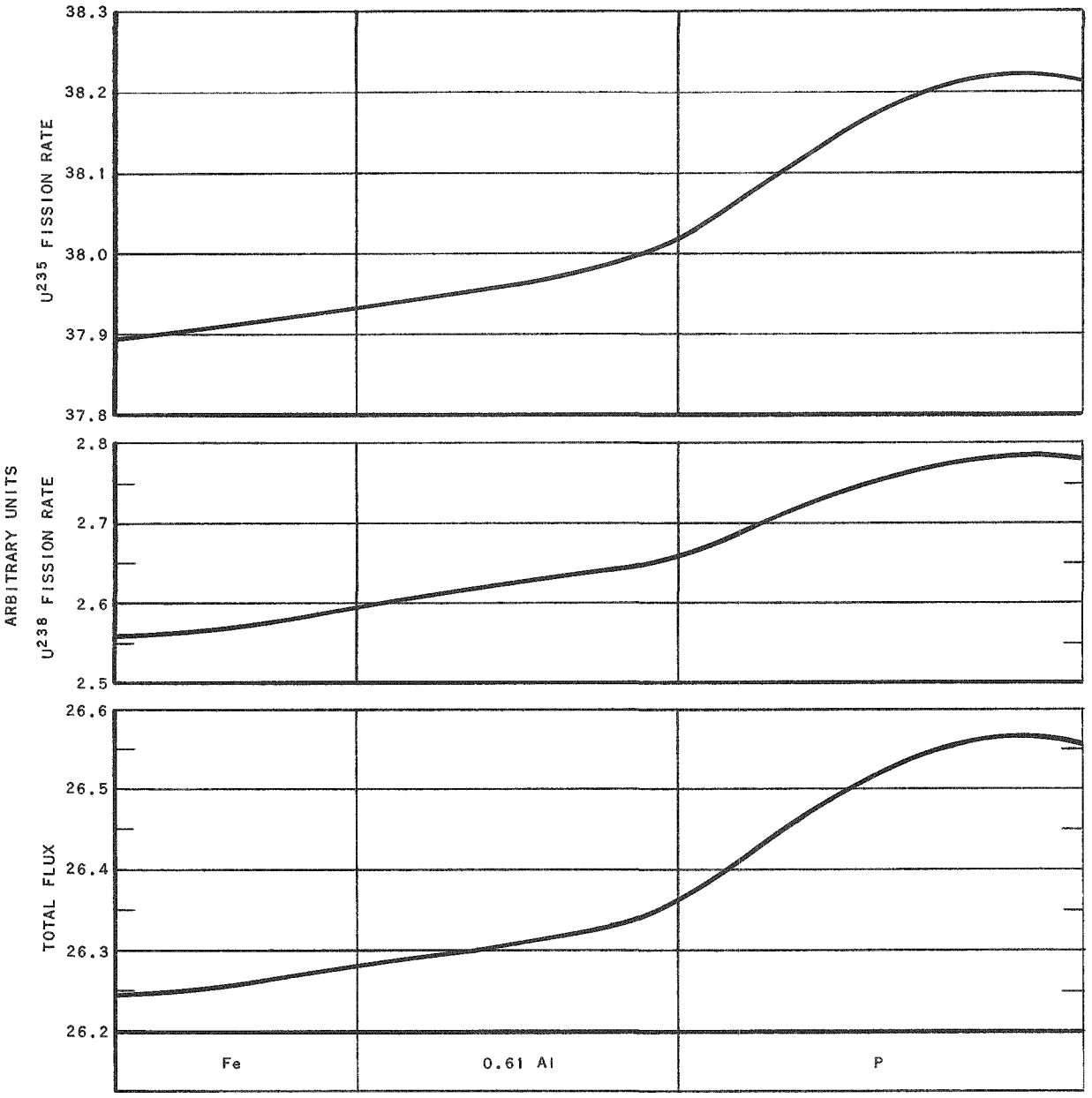

RE-7-19636-B

FIG. 29
SPATIAL DISTRIBUTION OF FISSION RATES AND TOTAL FLUX
(PBR ANALYSIS: PROBLEM NO. 17)

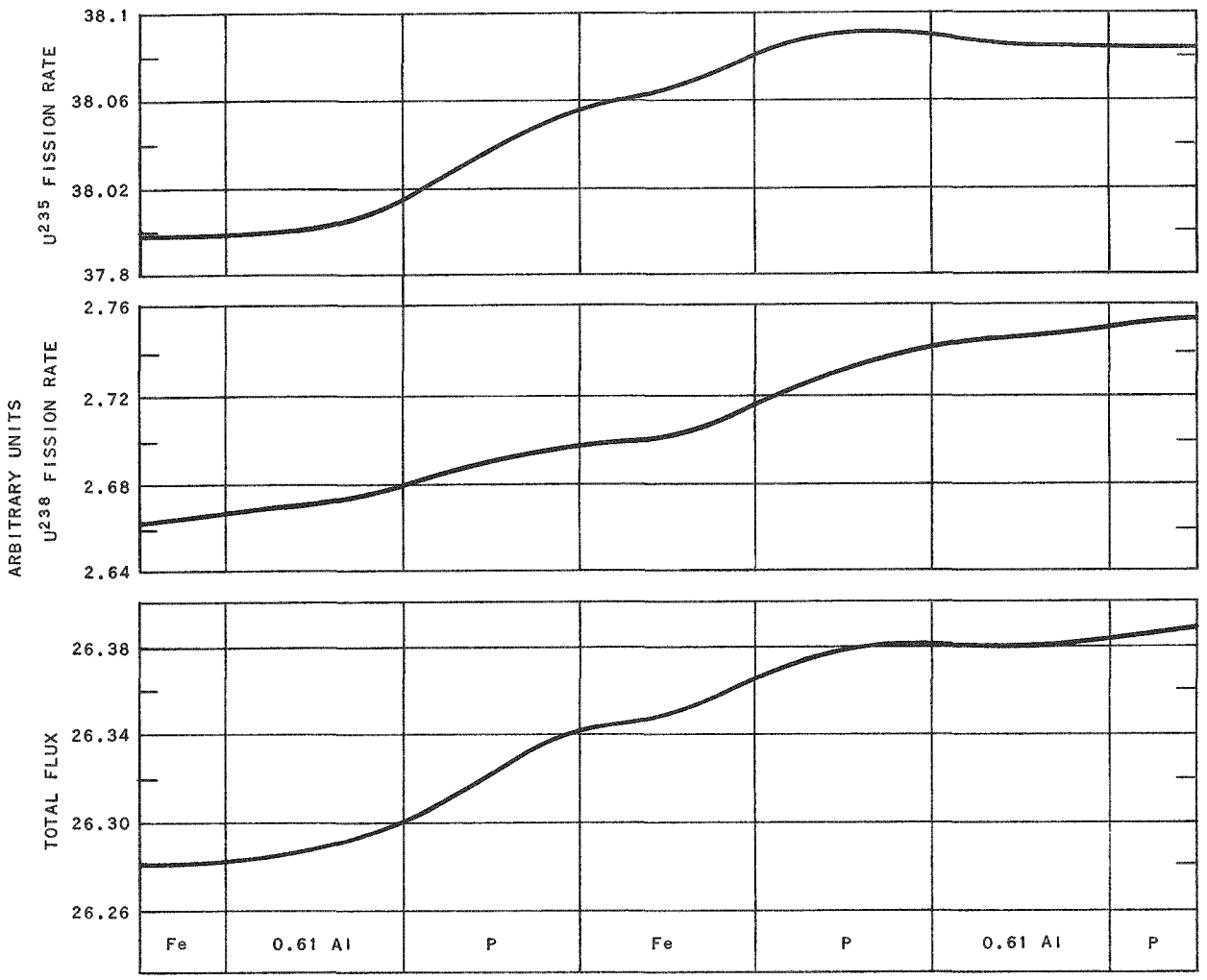

RE-7-19645-B

FIG. 30
SPATIAL DISTRIBUTION OF FISSION RATES AND TOTAL FLUX
(PBR ANALYSIS: PROBLEM NO. 18)

8. Conclusions

The rather good agreement between theory and experiment on calculations representing Assemblies 2, 2A, 2C and 2E suggests that one may confidently use this type of analysis to make qualitative predictions concerning inhomogeneities in proposed assemblies. Indications are that quantitative predictions may also be made.

Acknowledgements

The numerical work in compiling Table I and the plotting of the graphs were done by S. Dean, W. McCurdy and M. Schlapkohl.

The cooperation of Bengt Carlson and Janet Bendt at Los Alamos Scientific Laboratory is greatly appreciated.

B. Effect of High Temperature on Irradiated Fissium Alloy

R. J. Schiltz, E. S. Sowa

A series of tests were conducted in which cast 4% fissium alloy pins were taken from an irradiated fuel element (CP-5-7)[4] and heated to high temperatures.

The fuel had been irradiated to an estimated burnup of 1% of total atoms. This test was conducted to determine what effects could be expected in EBR-II fuel elements, after burnup, in the event of overheating for a short period.

Two samples (Nos. 1 and 4) were inserted in short lengths of standard EBR-II fuel element tubing (Type 304 stainless steel, 0.156 in. ID. by 0.008 in. wall thickness). They were heated to a temperature below the melting point (approximately 1335F) of the U-Fe eutectic to avoid melting of the test specimen. Samples No. 2, 3, and 5 were heated in ceramic tubes to 1825F.

The heating was conducted in a vertical, cylindrical furnace with resistance heaters placed around the external circumference. The samples were placed in a pedestal within the furnace and a purging flow of argon was admitted into the top. The gas flowed down over the sample and

---

[4] Reactor Engineering Division Quarterly Report - Section II, ANL-5601 (July, 1956).

out through a hole in the bottom of the furnace. The furnace temperature was measured by a thermocouple in a stainless steel tube inserted through the furnace top and situated just above the sample.

The results are listed in Table II.

Table II

HEATING TESTS ON CP-5-7 FISSIUM ALLOY PINS

Sample	Temperature, F	Time at Temperature, min.	Container	Diameter, in. Before Heating	Diameter, in. After Heating	Condition
1	1300	10	Stainless Steel	<0.156	0.156	Specimen stuck slightly in tube.
2	1825	10	Ceramic	0.142	0.192	Center hollowed out after heating.
3	1825	10	Ceramic	0.142	0.189	Piece solid but expanded.
4	1275 - 1290	10	Stainless Steel	0.148	0.156	Removed from tubing with difficulty.
5	1275 - 1290	10	Ceramic	-	-	Stuck in furnace.

In each case the pins expanded in diameter until confined by their container. Sample No. 5 could not be removed from the furnace; consequently, measurements could not be made on its diameter after heating.

The expansion of the pin is believed to be due to the expansion of fission gases in the metal and the reduced strength of the metal at the higher temperatures. Sample No. 2 appeared to have formed a "gas pocket" which forced the metal from the center of the sample.

These results indicate that expansion of the burned-up fuel will occur if exposed to temperatures of 1300F or above for relatively short periods of time.

C. Evaluation of Gears and Bearings for Service in High - Temperature Sodium
A. R. Jamrog, R. A. Stella

The EBR-II design requires operation of certain fuel-handling mechanisms submerged in high-temperature sodium. Fig. 31 shows schematically the apparatus used to evaluate the performance of gears and bearings in sodium at temperatures, loads, and speeds characteristic of the fuel-handling equipment operation.[5]

The test results (Tables III to V) indicate that certain gears, shaft and bearing combinations are available which operate successfully in the simulated EBR-II environment.

D. Bellows Seal and Sodium Condensation Test - E. Hutter, O. S. Seim

The welded stainless steel bellows[6] failed after completing approximately 40,000 full cycles at room temperature, and with an internal argon pressure of 15-30 in. H_2O. The failure was in the form of a crack which developed adjacent to a weld joining the peripheries of two disks (see Fig. 32).

A bellows of similar design will be used on the EBR-II control mechanisms. On the basis of this single test, it appears that such a bellows probably is well suited for this application; however, further tests will be conducted.

Visual inspection of the shaft test sections after a 37-day operating period revealed no increase in the rate of build-up of sodium due to condensation over that previously reported in ANL-5601: 0.09 in./yr at a point one foot above the sodium level.

E. Sodium-Air Reaction Experiments - J. R. Humphreys

One factor which enters into the design of a containment vessel for EBR-II is the magnitude of the pressure build-up within the vessel due to a reaction between sodium and air in the remote event that a nuclear incident resulted in ejection of primary tank sodium into the reactor building (containment vessel). Initial experiments directed toward determination of such pressure transients have been conducted in which varying quantities of sodium at 750F were expelled from a reservoir into a reaction vessel by detonation of a hydrogen-oxygen gas mixture.

---

[5] Reactor Engineering Division Quarterly Report, ANL-5371, January 15, 1955, p. 223.

[6] Reactor Engineering Division Quarterly Report - Section II, ANL-5601 (July, 1956).

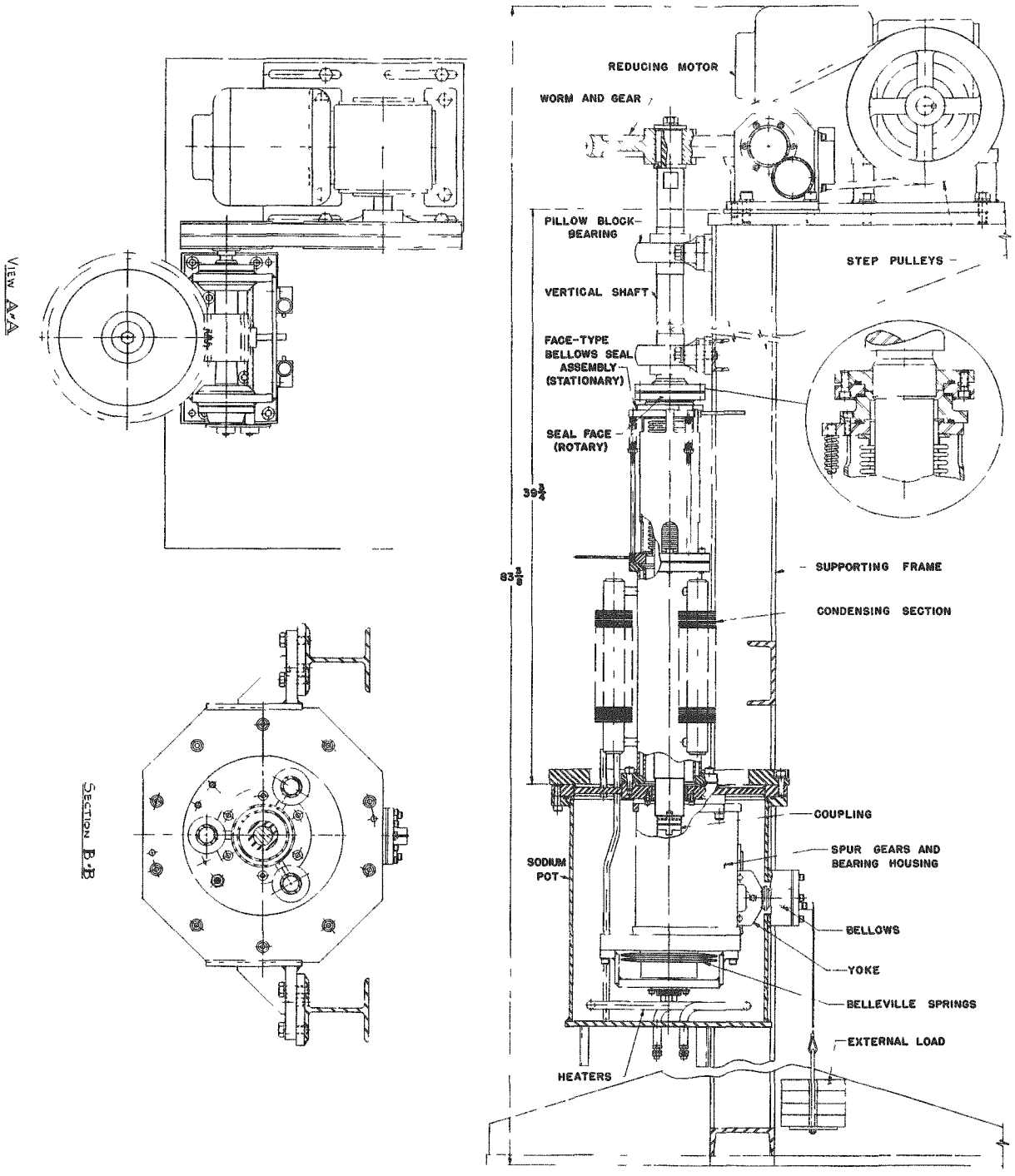

FIG. 31
TEST APPARATUS USED TO EVALUATE
ROTARY SEALS, GEARS AND BEARINGS
FOR LIQUID METAL-COOLED SYSTEMS

Table III

SUMMARY OF GEAR TEST IN LIQUID SODIUM[3]

Gear Speed: 8.6 rpm

Gear Description		Hardness, Rockwell C	Test Temperature, F	(A)[1] Oil Lube Load Rating, lb	(B) Applied Test Load, lb	B/A (x100)	Test Time, hr	Total Revolutions	Total Starts
Type	Material								
American Standard 20-deg Stub Tooth; 12 in. diametral pitch 36 teeth; 1 in. face	SAE 4640,(CP)[2]	52	300	1110	28	2.5	445	211,461	105,730
			400	1110	85	7.6	2	950	480
			300	1110	56	5.0	1852	851,000	425,500
	SST 440C,(CP)	48							
American Standard 14.5-deg full depth; 10 in. diametral pitch 30 teeth; 1 in. face	Tantung G	56	900	1000	28	2.8	208	75,500	47,750
			900	1000	42.5	3.8	426	195,278	97,639
		57							
American Standard 20-deg Stub Tooth; 12 in. diametral pitch 36 teeth; 1 in. face	High Speed Tool Steel (CP)	55	900	1110	42.5	3.8	956	438,230	169,115
		54							

[1]Using Lewis Formula: $W = Fsyc/P_d$. (s = stress; assumed 300,000 psi for heat treated gear steel).

[2](CP) = chrome plated.

[3]Over-all Evaluation: No visible wear.

Table IV

SUMMARY OF BALL BEARING TESTS IN LIQUID SODIUM AND SODIUM VAPOR

Bearing Description	Material: Races & Balls	Material: RC	Material: Retainer	Material: RC	Test Temperature, F	Thrust Load, lb	Radial[1] Load, lb	Test Time, hr	Race Displacement,[3] in.: Before	Race Displacement,[3] in.: After	Appearance
Angular Contact;New Departure #20208-#5A; 1.5748 in. bore; 3.1496 in. OD; 11 balls, 15/32 in. dia.	Stellite 3	56	Berylco 255	44	300	90	14	445	0.002	0.008	Copper smear on balls and races.
		56		43	300	90	14	445	0.002	0.009	
Angular Contact;New Departure #20208-#5A; 1.5748 in. bore; 3.1496 in. OD; 15 balls, 15/32 in. dia.	Stellite 3	57	None		400	240	42.5	2.5	0.0025	0.0025	No evidence of bearing wear.
					300	240	28	1852	0.0025	0.0035	Slight tarnish.
		57	None		400	240	42.5	2.5	0.0025	0.0025	No evidence of bearing wear.
					300	240	28	1852	0.0025	0.0035	Slight tarnish.
		54	None		900	240	21	956	0.0015	0.0063	Dark tarnish.
		57	None		900	240	21	956	0.0015	0.0053	Dark tarnish.
Angular Contact;[2] New Departure #20208-#5A; 1.5748 in. bore; 3.1496 in. OD; 15 balls, 15/32 in. dia.	Stellite 3	57	None		900	Misaligned during test. No load	>200	956	0.0035	-0.0032	Coated with Na and NaO No apparent damage.

[1]Calculated load based on friction coefficient of 0.8 at journal bearings.

[2]Tested in sodium vapor.

[3]Measure of over-all wear for angular contact bearing.

Table V

SUMMARY OF TESTS ON VARIOUS JOURNAL BEARING - SHAFT COMBINATIONS IN LIQUID SODIUM

Material Combination and Test Conditions	Bearing No.	Clearance, in. Initial	Clearance, in. Final	Wear, in.	Rockwell C Hardness Bearing Before	Rockwell C Hardness Bearing After	Rockwell C Hardness Shaft Before	Rockwell C Hardness Shaft After	Appearan
Bearing: Berylco 25S Shaft: SST 416, (CP) Test Temp: 300F Radial Unit Bearing Press.: 63.5 psi Total Revolutions: 211,461 No. of Starts: 105,730 Test Time: 445 hr	J-1	0.0012	0.001	+0.0002	44	44	37	37	Copper smear on shaft
	J-2	0.0012	0.0011	+0.0001	43	43	37	37	
	J-3	0.0012	0.001	+0.0002	43	43	37	37	
	J-6	0.0012	0.0012	0.0	43	43	37	37	Copper smear on shaft
Bearing: Berylco 10 Shaft: SST 416 (CP) Test Temp.: 400F Radial Unit Bearing Press.: 190.6 psi Total Revolutions: 950 No. of Starts: 480 Test Time: 2.5 hr	J-9	0.0024	-	-	24	24	40	40	Bearing galled badly
	J-10	0.0026	-	-	23	24	41	41	Good
	J-11	0.0026	-	-	23	23	40	40	Bearing galled badly
	J-12	0.0026	-	-	24	24	41	41	Bearing galled and seized
Bearing: High-Speed Tool Steel, (CuP) Shaft: High-Speed Tool Steel, 18-4-1, (CP) Test Temp.: 900F Radial Unit Bearing Press.: 63.5 psi Total Revolutions: 75,500 No. of Starts: 47,750 Test Time: 208 hr	J-13	0.0018	0.0008	+0.001	61	62	61	62	Bearing galled and seized
	J-14	0.0009	0.0008	+0.0001	63	63.5	61	62	Copper plating worn away in loaded region
	J-15	0.0008	0.0012	-0.0004	64	63	60	63	Copper plating continuous; no wear marks
	J-16	0.00084	0.0015	-0.00065	64	63.5	60	63	Copper plating worn away; bearing had begun to gall
	J-17	0.0004	0.0010	-0.0006	64	64	60	63	Copper plating worn off slightly. Galling at wear areas
	J-18	0.0007	0.0013	-0.0006	62	57	60	63	Bearing galled and seized
Bearing: Berylco 25 S Shaft: SST 416, (CP) Test Temp.: 300F Radial Unit Bearing Press.: 127 psi Total Revolutions: 851,000 No. of Starts: 425,500 Test Time: 1852 hr	J-5	0.0032	0.0045 0.0008	+0.0013 -0.0024	44	44	40	41	Copper smear on shaft
	J-3	0.0032	0.0014 0.0036	+0.0004 -0.0018	45	45	40	41	
	J-20	0.0031	0.0029 0.0046	+0.0002 -0.0015	25	23	40	41	
	J-19	0.0030	0.0055 0.0093	-0.0025 -0.0063	24	24	40	41	Copper smear on shaft
Bearing: High-Speed Tool Steel, (CP) Shaft: High-Speed Tool Steel, (CP) Test Temp.: 900F Radial Unit Bearing Press.: 95.3 psi Total Revolutions: 195,278 No. of Starts: 97,639 Test Time: 426 hr	J-21	0.0023	0.0015 0.0002	+0.0008 +0.0021	64	64	55	56	Satisfactory
	J-22	0.0023	0.0018 0.00045	+0.0005 +0.0018	63 61	61 59	56	56	
	J-23	0.0021	0.0021 0.0006	0.0 +0.0015	63 62	60 61	37	37	
	J-24	0.00193	0.0004 0.0019	+0.0003 +0.00153	64	64	43	42	
Bearing: HSTS, (CP); Radial Copper Pins Shaft: High-Speed Tool Steel, (CP) Test Temp.: 900F Radial Unit Bearing Press.: 115 psi Total Revolutions: 195,278 No. of Starts: 97,639 Test Time: 426 hr	J-37	0.00195	0.0015 0.0009	+0.00043 +0.00105	57	60	57	57	
	J-38	0.0018	0.0012 0.00185	+0.0006 -0.00005	60	60	57	57	Satisfactory
Bearing: HSTS, (CP); Longitudinal Copper Pins Shaft: High-Speed Tool Steel, (CP) Test Temp: 900F Radial Unit Bearing Press.: 190.6 psi Total Revolutions: 438,230 No. of Starts: 169,115 Test Time: 956 hr	J-39	0.0023	0.0006 0.0017	+0.0017 +0.0006	60	57	54 57	56	Satisfactory
	J-40	0.002	0.0055 0.0067	-0.0035 -0.0047	62	62	54 57	57	
Bearing: Stellite 3 Shaft: High-Speed Tool Steel, (CP) Test Temp.: 900F Radial Unit Bearing Press.: 95.3 psi Total Revolutions: 438,230 No. of Starts: 169,115 Test Time: 956 hr	J-1	0.0026	0.0025 0.0019	+0.0001 +0.0007	61	56	54 57	59	
	J-2	0.0024	0.0056 0.0041	-0.0024 -0.0017	57.5	56	54 57	56	Satisfactory

Note: (CP) = Chrome Plated (CuP) = Copper Plated

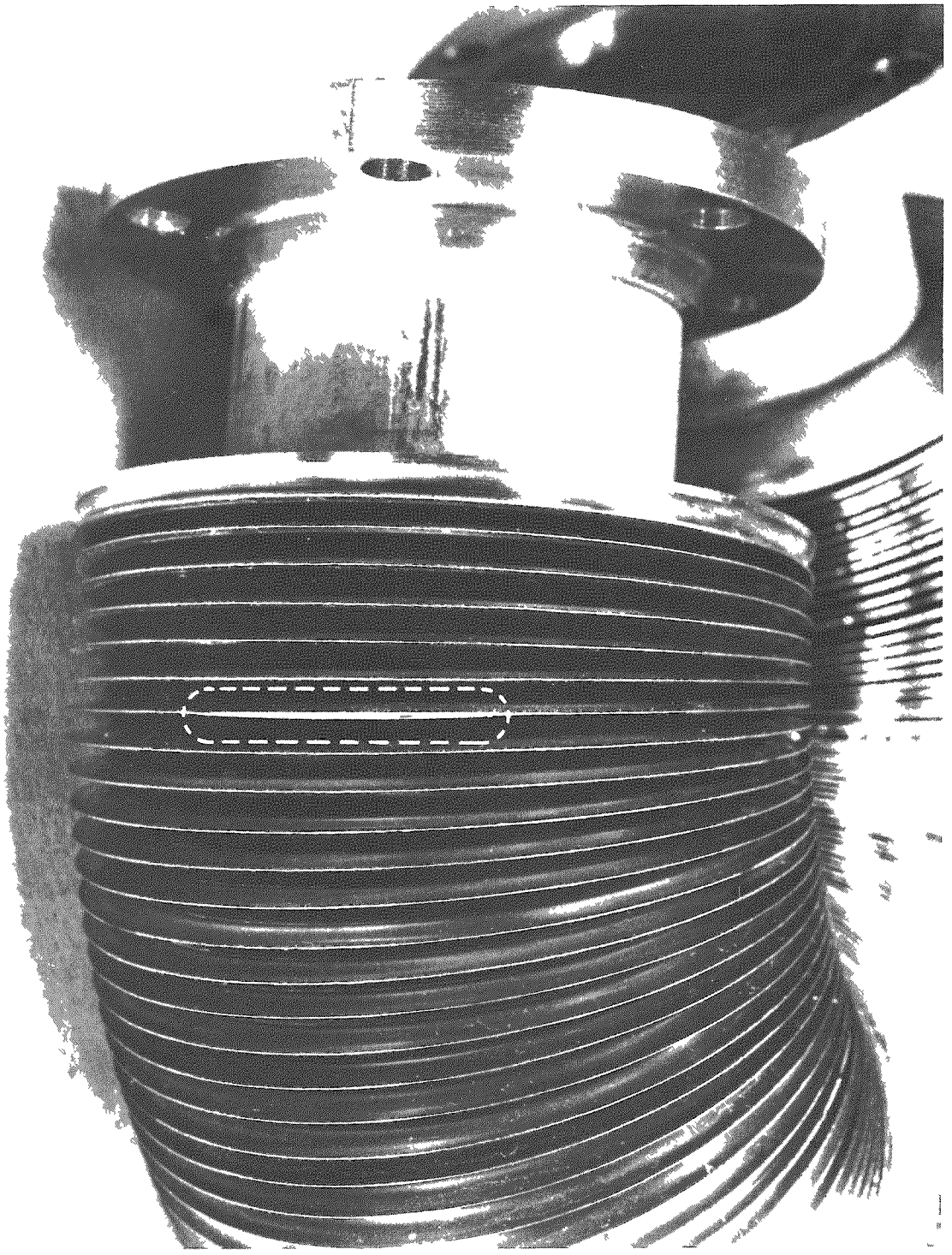

FIG. 32
BELLOWS FAILURE WHICH OCCURRED AFTER 40,000 CYCLES AT ROOM TEMPERATURE, WITH INTERNAL ARGON GAS PRESSURE OF 15-30 in H_2O

The reaction vessel was a 5-foot length of 8-inch Schedule 40 steel pipe (see Fig. 33). The "mortar" subassembly contained the reservoir of heated sodium as the top section directly above the hydrogen-oxygen ignition chamber (see Fig. 34). The sodium reservoir was sealed from the reaction vessel by a thin, aluminum rupture disk and was separated from the hydrogen-oxygen ignition chamber by a thin stainless steel rupture disk. When the hydrogen-oxygen mixture was detonated by a spark, the contents of the sodium reservoir were explosively ejected into the reaction vessel. Pressure measurements were made using a Pressuregraph variable capacitance pressure transducer and amplifier. The pressure signal was transmitted to an oscilloscope and photographed.

In the test series, varying amounts of sodium were introduced to the reaction vessel. In all cases oxygen was present in excess. Quantities of sodium added are reported in Table VI as a percentage of the necessary amount of sodium required for stoichiometric reaction with the atmospheric oxygen contained in the reaction vessel to form sodium monoxide. Test results are shown in Table VI. The quantity of sodium added is the only variable. In all cases, the measured values of peak pressures were considerably lower than the theoretical maximum pressure rise. The theoretical maximum pressure rise was calculated on the basis of complete reaction of sodium with oxygen to form sodium monoxide; the heat of reaction was assumed to be transferred completely to the residual atmospheric gases. It will be noted that the differences between the measured and the theoretical differential pressures increase with increasing quantities of sodium.

A portion of the measured peak pressure rise was due to the hydrogen-oxygen reaction plus the heat of reaction of the resulting water vapor with sodium. To measure this effect, the experiments in which the loadings of sodium were 27% and 54% were repeated with an atmosphere of argon in the reaction vessel. Pressure rises of 7 and 10 psi were measured for the 27% sodium loading, and 5 and 7 psi were measured for the 54% loading. Thus, in the 25% loading about 13 - 18% of the measured pressure rise is attributable to the sodium-injection reactions, with 5 to 10% increase for the 54% loading. The added effect in the case of the 13% loading would be comparable to the 27% loading values, and the 40% and 67% loadings comparable to the 54% values.

Previous work has shown an apparent influence of humidity upon the kindling temperature of sodium. To test this effect on the peak pressures, the 54% loading was repeated with dry air in the reaction vessel. Peak pressures of 50 and 64 psi were recorded for these dry air runs, comparing with 67, 70 and 78 psi for the runs using air containing about 60% relative humidity at 80F. On the basis of these data, there appeared to be a small influence of humidity on the peak pressure.

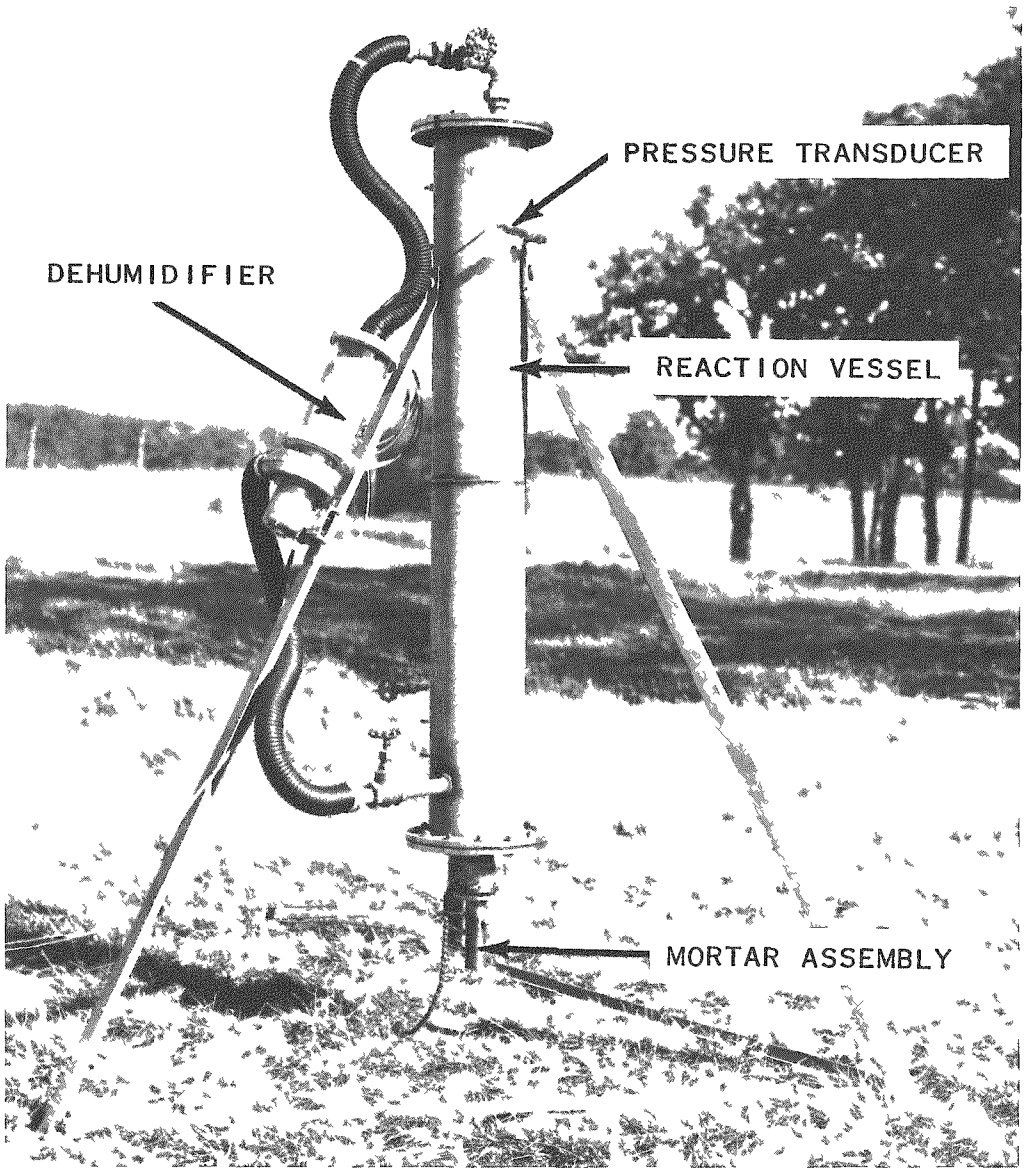

FIG. 33
SODIUM-AIR REACTION TEST FACILITY

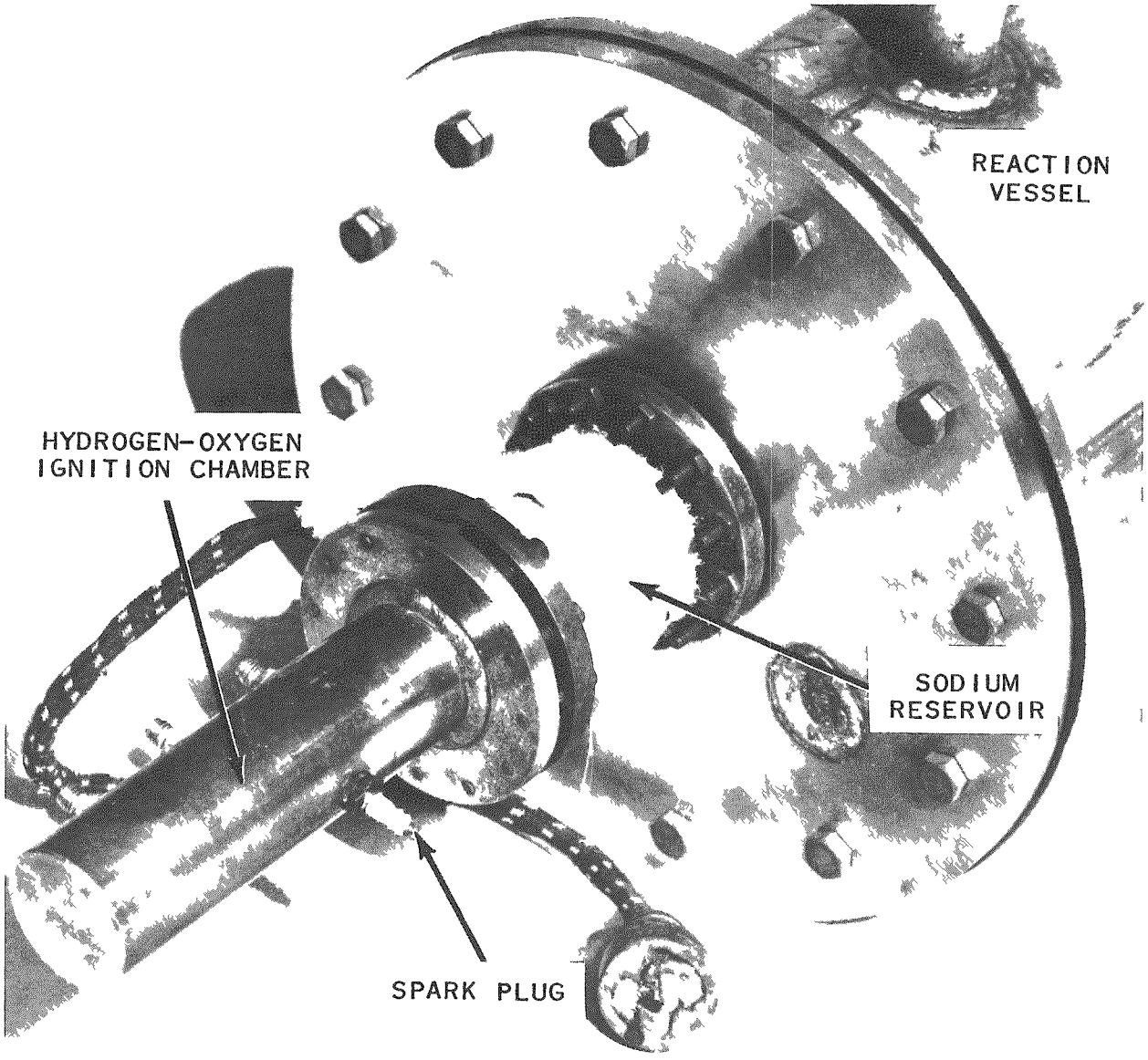

FIG. 34
MORTAR SUBASSEMBLY

Table VI

PEAK PRESSURE VARIATION WITH SODIUM QUANTITY

Quantity of Sodium, %	Pressure Rise, psi	
	Theoretical (Max.)	Measured (Peak)
13	70	33
		36
27	120	44
		55
		55
40	180	55
		66
		83
		92
54	240	67
		70
		78
67	300	70
		75

The particle size of the ejected sodium for a given sodium loading will determine the surface area of sodium available for reaction with oxygen. As the rate of reaction is proportional to the sodium surface exposed, this will influence the degree of sodium reaction during the time-of-flight period. The particle size of the sodium will be determined by the intensity of the hydrogen-oxygen ejection explosion and by the degree of atmospheric violence encountered in the reaction vessel as a result of the addition of large quantities of heat to the gas region immediately over the mortar assembly. Three 54% runs were made using 1.5 times as much hydrogen and oxygen for the propulsion reaction to achieve better initial mechanical dispersion of the sodium. Peak pressures of 88, 94 and 100 psi were obtained indicating that better mechanical dispersion does increase the maximum pressure values to a greater extent than could be explained by the 300 calories added by the additional hydrogen-oxygen-sodium reactions.

In all runs, the pressure profiles were similar in shape. Figure 35 shows two typical pressure transients. It will be observed that the peak pressures occur within the 6 to 15-millisecond sodium time-in-flight period. This is what would be expected in the case of very high temperature gas contained in a cold vessel. A rapid pressure drop occurs as heat is lost to the

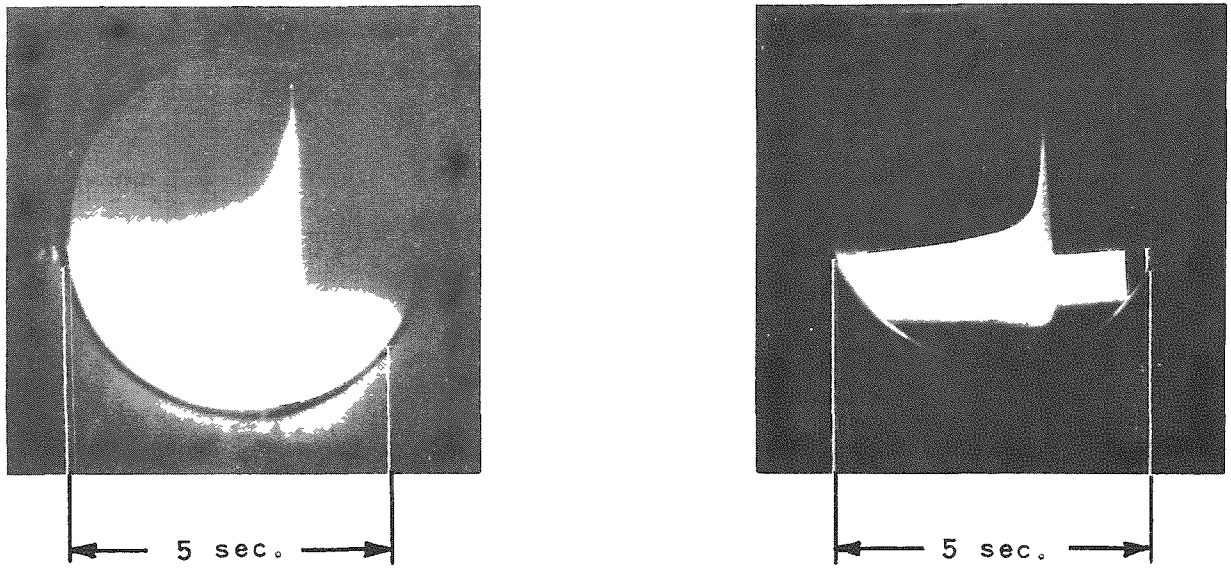

54% SODIUM — LOADING — 54% SODIUM

REL. HUMIDITY: 47.5% AT 85 F — VESSEL ATM. — DRY AIR

$1.5(2H_2 + O_2)$ — PROPELLENT — $1.0(2H_2 + O_2)$

88 psi — PEAK PRESSURE — 64 psi

FIG. 35
TYPICAL OSCILLOGRAPHIC PRESSURE TRANSIENT CHARACTERISTICS

tank walls, the decrease becoming slower as the temperature of the tank walls increases and the rate of heat loss from the gas is reduced. This sequence of heat transfer occurs very rapidly in the small system, but would be slowed down considerably in a large system, such as the EBR-II containment building, due to the much smaller vessel-to-air heat capacity ratio and the much larger mean-distance-to-wall figure. A peak pressure enduring for a matter of milliseconds in this small experimental vessel would be expected to last much longer in a full-scale containment model.

In order to observe the large-system effects, a second series of experiments are to be conducted using a containment tank 3 feet in diameter and 10 feet in height. Sodium injections up to 100% stoichiometric quantities are planned.